



Spatiotemporal dynamics of surface sediment characteristics and benthic macrofauna compositions in a temperate high-energy River-dominated Ocean Margin

Bastien Lamarque, Bruno Deflandre, Sabine Schmidt, Guillaume Bernard, Nicolas Dubosq, Melanie Diaz, Nicolas Lavesque, Frederic Garabetian, Florent Grasso, Aldo Sottolichio, et al.

► To cite this version:

Bastien Lamarque, Bruno Deflandre, Sabine Schmidt, Guillaume Bernard, Nicolas Dubosq, et al.. Spatiotemporal dynamics of surface sediment characteristics and benthic macrofauna compositions in a temperate high-energy River-dominated Ocean Margin. Continental Shelf Research, 2022, 247, pp.104833. 10.1016/j.csr.2022.104833 . hal-03866642

HAL Id: hal-03866642

<https://hal.science/hal-03866642>

Submitted on 23 May 2023

HAL is a multi-disciplinary open access archive for the deposit and dissemination of scientific research documents, whether they are published or not. The documents may come from teaching and research institutions in France or abroad, or from public or private research centers.

L'archive ouverte pluridisciplinaire **HAL**, est destinée au dépôt et à la diffusion de documents scientifiques de niveau recherche, publiés ou non, émanant des établissements d'enseignement et de recherche français ou étrangers, des laboratoires publics ou privés.



Distributed under a Creative Commons Attribution - NonCommercial - NoDerivatives 4.0 International License

Spatiotemporal dynamics of surface sediment characteristics and benthic macrofauna compositions in a temperate high-energy River-dominated Ocean Margin

Bastien Lamarque ^{1, *}, Bruno Deflandre ², Sabine Schmidt ², Guillaume Bernard ¹, Nicolas Dubosq ², Mélanie Diaz ^{2, **}, Nicolas Lavesque ¹, Frédéric Garabetian ¹, Florent Grasso ³, Aldo Sottolichio ², Sylvain Rigaud ⁴, Alicia Romero-Ramirez ¹, Marie-Ange Cordier ², Dominique Poirier ², Martin Danilo ² and Antoine Grémare ¹

¹ UMR EPOC, Université de Bordeaux, CNRS, UMR 5805, Station Marine d'Arcachon, 2 rue du Professeur Jolyet, 33120 Arcachon, France

² UMR EPOC, Université de Bordeaux, CNRS, UMR 5805, Bâtiments B18/B18N, Allée Geoffroy Saint-Hilaire, CEDEX, 33615 Pessac, France

³ IFREMER, DYNECO/DHYSED, Centre de Bretagne, CS 10070, 29280 Plouzané, France

⁴ Université de Nîmes, EA 7352 CHROME, rue du Dr Georges Salan, 30021 Nîmes, France

* Correspondence: bastien.lamarque@u-bordeaux.fr

** Present address: Royal Netherlands Institute for Sea Research, Department of Coastal Systems, and Utrecht University, PO Box 59, 1790 AB Den Burg Texel, The Netherlands

Abstract:

The benthic compartment of River-dominated Ocean Margins (RiOMar) is largely affected by sedimentary processes, as well as by natural and anthropogenic disturbances. Recent studies have confirmed the major importance of riverine inputs and local hydrodynamics in the spatial structuration of low- and high-energy temperate RiOMar, respectively. Differences in the nature of these structuring factors could also affect the temporal dynamics of these two types of systems. The present study is aiming at: (1) quantifying spatiotemporal changes in surface sediment and benthic macrofauna within the West Gironde Mud Patch (WGMP; high-energy system) over both short (2016-2018) and longer (2010/2016-2018) time scales, (2) identifying the main environmental factors explaining those changes, and (3) achieving a comparison with the Rhône River Prodelta (RRP; low-energy system) in view of further characterizing the functioning of the benthic components of these two temperate RiOMar. Surface sediment characteristics (grain size, quantitative and qualitative descriptors of particulate organic matter) and benthic macrofauna compositions were assessed based on 4 seasonal sampling of 5 stations located along a depth gradient within the WGMP. Results highlighted the existence of spatial patterns for both surface sediment and benthic macrofauna, which are both better explained by local hydrodynamics. Most variables presented seasonal changes. Benthic macrofauna compositions also showed pluri-annual changes, which were attributed to a cicatrization process following a major disturbance caused by the 2013-2014 series of severe winter storms, and suggests the major role of local hydrodynamics in

explaining 2010/2016-2018 temporal changes in WGMP benthic macrofauna compositions. The comparison with the RRP further highlighted major discrepancies between the two systems in the main processes (i.e., hydrodynamics *versus* river hydrological regime) explaining surface sediment characteristics and benthic macrofauna compositions, which supports current RiOMar typologies.

Keywords: RiOMar; West Gironde Mud Patch; North-East Atlantic shelf; Particulate organic matter; Benthic macrofauna; Spatiotemporal changes; Hydrodynamics; Storms

Abbreviations:

AFDW : Ash-Free Dry Weight

AJD : Annual Julian Days

BSS : Bottom Shear Stress

BSS₁₀₀ : Bottom Shear Stress integrated over 100-day periods

BSS₃₆₅ : Bottom Shear Stress integrated over 365-day periods

Chl-*a* : Chlorophyll-*a*

CJD : Cumulated Julian Days

D_{0.5} : Median diameter of sediment particles

dbRDA : distance-based Redundancy Analysis

DISTLM : DISTance-based Linear Model

DW : Dry Weight

EHAA : Enzymatically Hydrolysable Amino Acids

Flow₁₀₀ : River flows integrated over 100-day periods

Flow₃₆₅ : River flows integrated over 365-day periods

nMDS : non-Metric Multidimensional Scaling

PCA : Principal Components Analysis

Phaeo-*a* : Phaeophytin-*a*

POC : Particulate Organic Carbon

POM : Particulate Organic Matter

RiOMar : River-dominated Ocean Margin

RRP : Rhône River Prodelta

SIMPROF : SIMilarity PROFile procedure

SSA : Sediment Surface Area

THAA : Total Hydrolysable Amino Acids

WGMP : West Gironde Mud Patch

1. INTRODUCTION

Continental margins are key areas for the marine component of major biogeochemical cycles, accounting for the mineralization of 50 to 80 % of continental Particulate Organic Carbon (POC) inputs (Aller, 1998; Blair and Aller, 2012; Burdige, 2005). Continental margins

1 impacted by major river freshwater and sediment discharges are defined as River-dominated
2 Ocean Margins (RiOMar). RiOMar provide a large variety of ecosystem services including
3 provisioning (e.g. fisheries), regulating (e.g. carbon mineralization/burial) and supporting (e.g.
4 nutrients cycling, habitats) ones (e.g. Aller, 1998; Levin et al., 2001; Lansard et al., 2009).
5 Their benthic components constitute the main marine primary depositional areas of riverine
6 particule inputs (Burdige, 2005; McKee et al., 2004) and it is estimated that RiOMar account
7 for 40 to 50 % of continental POC burial in continental margins (Blair and Aller, 2012; Burdige,
8 2005; Hedges and Keil, 1995). RiOMar benthic biological compartments (e.g. macrofauna)
9 and biogeochemical fluxes (e.g. mineralization) are largely affected by a variety of natural and
10 anthropogenic disturbances (Aller, 1998; Lansard et al., 2009; Lotze et al., 2006; Rhoads et al.,
11 1985; Tesi et al., 2007; Ulses et al., 2008; Worm et al., 2006).

12
13 The impact of both sediment discharges and associated organic matter inputs on the
14 structuration of benthic macrofauna communities and biogeochemical functioning of the
15 sediment-water interface has been documented for a large variety of RiOMar (Akoumianaki et
16 al., 2013; Aller and Aller, 1986; Aller and Stupakoff, 1996; Alongi et al., 1992; Bonifácio et
17 al., 2014; Harmelin-Vivien et al., 2009; Rhoads et al., 1985; Wheatcroft, 2006). Mostly based
18 on the analysis of macrofauna vertical distribution within the sediment column and X-ray
19 radiographies, Rhoads et al. (1985) first proposed a conceptual model describing the response
20 of benthic macrofauna and surface sediments to the inputs of major rivers. According to this
21 model, macrofauna spatial distribution is mainly controlled by the interaction between: (1) the
22 physical disturbance induced by intense riverine particles inputs, and (2) Particulate Organic
23 Matter (POM) availability. In proximal (i.e., the closest to the river mouth) parts of RiOMar,
24 high and irregular sedimentation rates induce sedimentary instability, precluding the
25 establishment of mature macrobenthic communities. The high turbidity of river plumes also
26 limits primary production in the water column, resulting in mainly low (refractory) POM
27 concentrations in surface sediments. Accordingly, RiOMar proximal areas are characterized by
28 low bioturbation intensities and low mineralization fluxes. Conversely, in distal (i.e., deeper)
29 parts, moderated sedimentation and enhanced primary production in the water column allow
30 for the establishment of mature macrobenthic communities, high bioturbation intensities and
31 mineralization fluxes.

32
33 More recent RiOMar typologies, based on meta-analyses (mostly achieved on tropical
34 and subtropical systems) of geomorphological and biogeochemical processes, highlighted the
35 major effect of local hydrodynamics on RiOMar morphologies and POC mineralization/burial
36 intensities (Blair and Aller, 2012; McKee et al., 2004). This led to a clear distinction between:
37 (1) low-energy systems, with both high sedimentation rates and carbon preservation (later
38 referred as type 1), and (2) high-energy tidal and/or wave systems with both high sediment
39 oxygenation and low carbon preservation rates (later referred as type 2). Lamarque et al. (2021)
40 recently assessed the main environmental factors responsible for the spatial structuration of
41 temperate type 1 and type 2 systems based on the comparison between extensive spatial surveys
42 conducted within the Rhone River Prodelta (RRP; type 1, French Mediterranean coast) and the
43 West Gironde Mud Patch (WGMP; type 2, French Atlantic coast). Their results confirmed the

major importance of riverine inputs and local hydrodynamics in the spatial structuration of type 1 and type 2 temperate RiOMar, respectively.

Such a difference in the nature of their main structuring factors could as well affect the spatiotemporal dynamics of these two types of systems. Seasonal changes in both surface sediment characteristics and benthic macrofauna compositions along a depth gradient have already been addressed within the RRP by Bonifácio et al. (2014). Results showed that temporal changes were larger at the most proximal station in relation with changes in river flows. Major changes were observed after a prolonged low-flow period, which allowed for the development of a mature macrobenthic community (otherwise precluded due to high sedimentation rates resulting from POM riverine inputs). Conversely, temporal changes in benthic surface sediment characteristics and benthic macrofauna compositions within the WGMP have only been poorly documented so far. The only available quantitative benthic macrofauna composition data have been collected during a single cruise and at only 3 stations (Massé et al., 2016). Consequently, the explaining factors and the magnitude of spatiotemporal changes in surface sediment characteristics and benthic macrofauna compositions within the WGMP (taken as an example of temperate type 2 RiOMar) are still largely unknown.

The present study is aiming at filling this gap by: (1) quantifying spatiotemporal changes in surface sediment characteristics and benthic macrofauna compositions within the WGMP over both short (2016-2018) and long (2010/2016-2018) time scales, (2) identifying the main environmental factors explaining these changes, and (3) achieving a comparison with the RRP. Main tackled questions were as follows: (1) What are the relative importance of spatial and temporal changes in both WGMP surface sediment characteristics and benthic macrofauna composition? (2) Are the factors better explaining spatial changes in WGMP sediment profile image characteristics and spatiotemporal changes in benthic macrofauna composition similar? (3) Are the differences between spatiotemporal changes in benthic macrofauna composition in the RRP and the WGMP compatible with their classification as type 1 and type 2 RiOMar?

2. MATERIALS & METHODS

2.1 WGMP: Sampling area

The West Gironde Mud Patch (WGMP) is a 420 km² sedimentary body located in the Bay of Biscay 40 km off the Mouth of the Gironde Estuary, between ca. 30 and 75m depth (Figure 1). This relict paleovalley is the primary depocenter (sedimentation rates between less than 1 and 10 mm.y⁻¹; Dubosq et al., 2021) of fine particles originating from the Gironde Estuary, which has an annual mean water flow of 944 m³.s⁻¹ (Doxaran et al., 2009) with daily flows up to 7,500 m³.s⁻¹ (Constantin et al., 2018). The WGMP is located in a macro-tidal environment with a tidal range from 1.5 to 5m (Jalón-Rojas et al., 2018). The continental shelf off the Mouth of the Gironde Estuary is periodically submitted to strong swells/waves, which can reach maximal amplitudes of 15 m and periods of 15 s (Cirac et al., 2000; Masselink et al.,

2016). The sedimentology of the WGMP has been extensively studied based on stratigraphic sequences, palynological data, X-ray radiographies and radiochronographies (Castaing et al., 1979, 1982; Castaing and Allen, 1981; Gadel et al., 1997; Jouanneau et al., 1989; Lesueur et al., 1991, 1996, 2001, 2002; Lesueur and Tastet, 1994; Longère and Dorel, 1970; Parra et al., 1998; Weber et al., 1991). These surveys have attributed a major role to local hydrodynamics in controlling the spatial structuration of the WGMP. This paradigm was based on both: (1) the segmentation between a proximal and a distal part with no modern persistent sedimentation in the former, and (2) the decreasing frequency of occurrence of vertical erosional sequences within the sediment column with station depth (Jouanneau et al., 1989; Lesueur et al., 1991, 2001, 2002; Lesueur and Tastet, 1994). It was recently further validated by a synoptic survey of the spatial distributions of surface sediment and sediment profile image characteristics (Lamarque et al., 2021).

2.2. WGMP: Sampling of surface sediment and benthic macrofauna

Five stations located along a depth gradient (Figure 1A, Table I) were sampled for surface sediment characteristics and benthic macrofauna during 4 cruises, which took place on board of the R/V Côtes de la Manche in October 2016 (Deflandre 2016), August 2017 (Deflandre 2017), February 2018 (Deflandre 2018a) and April 2018 (Deflandre, 2018b). This sampling design was set to document, over the whole WGMP, seasonally contrasted situations in terms of Gironde Estuary river flows and local hydrodynamics. Only 4 stations were sampled in February 2018 due to bad meteorological conditions. During each cruise, 4 sediment cores (10 cm internal diameter) were collected at each station using an Oktopus GmbH® multiple corer. The upper top 0.5 cm of each core was sliced and immediately frozen (-20°C) on board. A single core was used to assess sediment grain size, Sediment Surface Area (SSA; Mayer, 1994b), POC concentrations (hereafter POC) and $\delta^{13}\text{C}$. The remaining 3 cores were used to assess chloropigment and amino acid concentrations. Benthic macrofauna was sampled using a 0.25 m² Hamon grab (3 replicates), sieved on a 1 mm mesh and fixed with 4 % formalin.

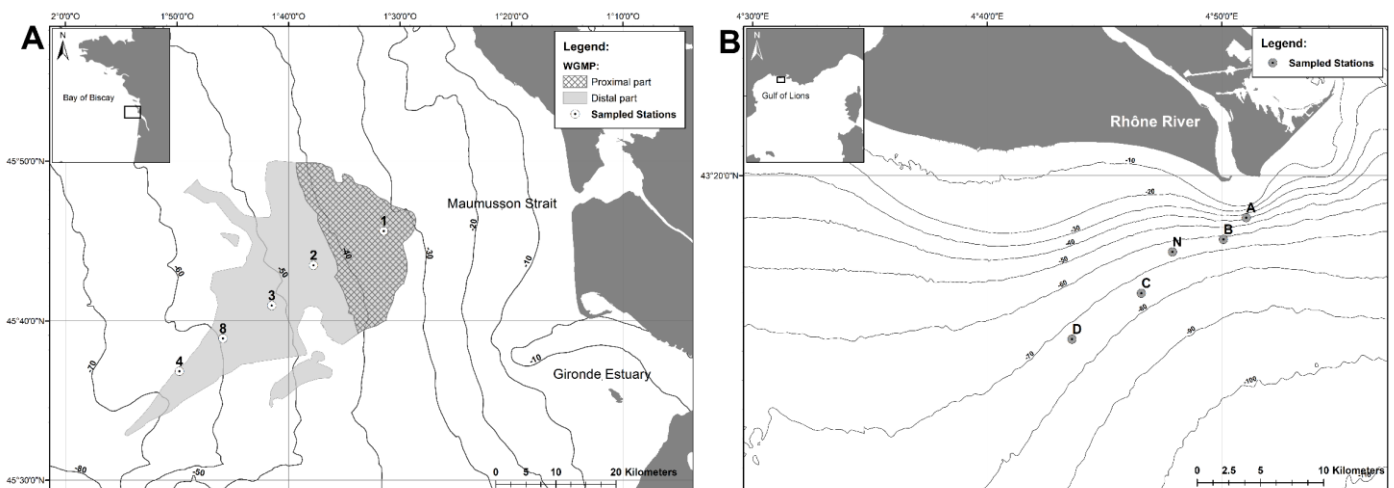


Figure 1. Sampling: Map showing the delimitation of: (A) the West Gironde Mud Patch (WGMP) along the French Atlantic Coast together with the locations of the 5 sampled stations. Stations 1, 3 and 4 had also been sampled in July 2010 by Massé et al. (2016); and (B) the

Rhône River Prodelta (RRP) in the Gulf of Lions (NW Mediterranean) together with the locations of the 5 stations sampled by Bonifácio et al. (2014) in April 2007, May and December 2008, and July 2011.

2.3. WGMP: Gironde Estuary water flows

Daily water flows of the Gironde Estuary were assessed by summing the flows of the Garonne and Dordogne Rivers. Data were downloaded at <http://www.hydro.eaufrance.fr>.

Table I. Sampling: Location (WGS84, degrees, and decimal minutes) and depth of the 5 stations (1, 2, 3, 8, 4) sampled in the West Gironde Mud Patch (WGMP) during the present study and of the 5 stations (A, B, N, C, D) sampled in the Rhône River Prodelta (RRP) by Bonifácio et al. (2014). (See text for details)

System	Station	Latitude (N)	Longitude (W)	Depth (m)
WGMP	1	45°45.580'	1°31.489'	37
	2	45°43.511'	1°37.773'	47.8
	3	45°41.007'	1°41.545'	56.5
	8	45°38.873'	1°45.777'	64.5
	4	45°36.924'	1°49.712'	71.5
RRP	A	43°18.690'	04°51.042'	24
	B	43°18.013'	04°50.068'	54
	N	43°17.626'	04°47.896'	67
	C	43°16.343'	04°46.565'	76
	D	43°14.917'	04°43.613'	74

2.4. WGMP: Local hydrodynamics

At each of the 5 sampled stations (Figure 1, Table I), daily values of Bottom Shear Stress (BSS) were computed from a tridimensional numerical model (Diaz et al., 2020; Grasso et al., 2018). This model is based on the MARS3D hydrodynamic model (Lazure and Dumas, 2008) and the WAVE WATCH III® wave model (Roland and Ardhuin, 2014) with a resolution of ca. 0.5x0.5 km² over the WGMP. The model integrates realistic hydro-meteorological forcing (i.e., wind, tide, surge and river flows). BSS were computed following Soulsby's

formulation (Soulsby, 1997). Simulations provided hourly outputs from 2010 to 2018 that were daily compiled and 95th percentiles were used to characterize BSS intensities accounting for intense hydrodynamic events.

2.5. WGMP: Surface sediment characteristics

Grain sizes were measured on aliquots of unreplicated sediment samples using a Malvern[®] Master Sizer laser microgranulometer. Almost all particle-size distributions were unimodal and therefore characterized through their median diameter ($D_{0.5}$). SSA was measured on unreplicated freeze-dried sediment samples, previously degassed overnight at 150°C, using a Gemini[®] VII Surface Area Analyzer (Micromeritics[®] 2390a model) with the multi-point Brunauer-Emmett-Teller method (Mayer, 1994b). POC were assayed using a LECO[®] CS 200 analyzer, after 2M HCl overnight decarbonation (Etcheber et al., 1999) of previously freeze-dried unreplicated sediment samples. They were normalized for SSA (i.e., expressed in terms of mass per SSA) since these two parameters were assessed on the same sediment core at each combination of stations*dates.

Total and Enzymatically Hydrolysable Amino Acids (THAA and EHAA) were analyzed on triplicates for each of the 3 sampled cores. THAA were extracted through acid hydrolysis (6M HCl, 100°C, 24h). EHAA were extracted following the biomimetic approach proposed by Mayer et al. (1995). THAA and EHAA were derivatized to form fluorescent amino compounds, which were separated by reverse phase High-Performance Liquid Chromatography (Agilent[®] 1260 INFINITY) on a Phenomenex[®] Kinetex 5 μ m EVO C18 column and detected using a 338 nm excitation wavelength. Their concentrations (hereafter THAA and EHAA) were expressed in terms of mass per mass of sediment Dry Weight (DW) since SSA were not measured on the same sediment cores.

Chlorophyll-*a* and Phaeophytin-*a* were assayed on unreplicated thawed frozen (-20°C) sediment samples after overnight acetone extraction (90 % final concentration) using a Perkin Elmer[®] LS-55 spectrofluorometer following Neveux & Lantoiné (1993). Their concentrations (hereafter Chl-*a* and Phaeo-*a*) were expressed in terms of mass per mass of sediment DW since SSA were not measured on the same sediment cores.

Chl-*a*/(Chl-*a* + Phaeo-*a*) ratios (hereafter Chl-*a*/(Chl-*a* + Phaeo-*a*)) were used as a lability index of vegetal biomass (Bonifácio et al., 2014; Pastor et al., 2011) and EHAA/THAA ratios (hereafter EHAA/THAA) were used as a lability index of bulk sedimentary organics (Bonifácio et al., 2014; Grémare et al., 2005; Medernach et al., 2001; Pastor et al., 2011; Wakeham et al., 1997).

For the analysis of POC isotopic ratio, duplicated freeze-dried sediment samples were decarbonated (1M HCl) and later analyzed using a Thermo Scientific[®] Delta V plus IRMS

coupled with a Thermo Scientific® Flash 2000 EA. Raw measurements were converted in usual $\delta^{13}\text{C}$ units (Coplen, 2011).

2.6. WGMP: benthic macrofauna

Macrofauna was sorted, identified to the lowest tractable taxonomic level and counted. Species richness was computed on pooled replicates for each combination of stations and dates. Biomasses (Ash-Free Dry Weights, AFDW) were measured for each individual taxon as ignition loss (450°C, 4 h) except for Ophiuridae for which an allometric regression was used to account for arm loss: $\text{AFDW} = 0.0111 \times (\text{disk diameter})^{2.5268}$ (where AFDW and disk diameter are expressed in g and mm, respectively; N. Lavesque, personal communication). Abundances and biomasses were standardized per m^2 .

2.7. WGMP: data analysis

To identify the most pertinent time scales for assessing the structuring role of river flows and local hydrodynamics on spatiotemporal changes in surface sediment characteristics (i.e., mean: SSA, POC/SSA, Chl-*a*, Phaeo-*a*, Chl-*a*/(Chl-*a*+Phaeo-*a*), THAA, EHAA, EHAA/THAA and $\delta^{13}\text{C}$) and benthic macrofauna compositions, the Pearson correlation coefficients linking their similarity matrices (Euclidean and Bray-Curtis distances, respectively) with similarity matrices based on either integrated river flows or integrated BSS were computed. This was achieved using R version 3.6.1 (R Core Team, 2019) with the additional packages vegan (Oksanen et al., 2019), BBmisc (Bischl et al., 2017) and Hmisc (Harrell, 2021) for river flows and BSS integrated over 1 to 365 days before each of the 4 cruises.

For the same surface sediment characteristics as described above, hierarchical clustering (Euclidean distance and average group linking) and Principal Components Analysis (PCA) were used to define groups of stations*sampling dates and to assess relationships between variables. A SIMilarity PROFile procedure (SIMPROF; Clarke et al., 2008) was used to test for the statistical significance of between-group differences. A DISTance-based Linear Model (DISTLM) was established to assess the potential contributions of river flows and BSS to spatiotemporal changes in surface sediment characteristics. This model was built using the Best selection procedure (Anderson et al., 2008) and the AIC selection criterion (Akaike, 1973). It was represented in a multidimensional space through a distance-based Redundancy Analysis (dbRDA; Anderson et al., 2008). All surface sediment analyses were performed on normalized data and river flows and BSS were integrated over both 100- (i.e., seasonal) and 365- (i.e., annual) day periods based on results of the above-described correlation analysis. Station depth, Annual Julian Days (i.e., AJD: the number of days since the beginning of the sampling year), and Cumulated Julian Days (i.e., CJD: the number of days since the first day

of the October 2016 cruise) were introduced as supplementary variables. The same approach was used for benthic macrofauna abundances (square-root transformed data). However, in this case and because of the use of the Bray-Curtis similarity, a non-Metric Multidimensional Scaling (nMDS) was achieved instead of a PCA. Moreover, an intermediate DISTLM/dbRDA was achieved using macrofauna composition as response variable and normalized surface sediment characteristics as predictor variables. POC, Phaeo-*a* and EHAA were excluded from this last procedure due to their strong correlation with other surface sediment characteristics.

A comparison was achieved with macrofauna abundance data collected in July 2010 at stations 1, 3 and 4 (i.e., station E, C and W in Massé et al., 2016) using exactly the same methodology (sampling gear and design, sorting procedure). Macrofauna identification was achieved at the same taxonomic resolution by the same Research group as well. Nevertheless, to avoid inconsistencies in taxa identification between the two studies, benthic macrofauna data were degraded at the genus level. The comparison was achieved through hierarchical clustering (square-root transformed data, Bray-Curtis distance and average group linking) and nMDS together with the SIMPROF procedure.

All multivariate analyses were computed using the PRIMER® 6 software package (Clarke and Warwick, 2001) with the PERMANOVA+ add-on (Anderson et al., 2008).

2.8. Comparison between the WGMP and the RRP

Intra-station temporal variabilities (i.e., among sampling dates considering each station individually) in sediment surface characteristics and benthic macrofauna compositions were compared in the WGMP (4 cruises between 2016 and 2018 as described above) and the RRP. The latter was sampled by Bonifácio et al. (2014), using the same approach and methodology as in the present study. More specifically, 5 stations located along a depth gradient from the mouth of the Rhone River, taking into account the preferential direction of its plume (Figure 1B; Table I), were sampled during 4 cruises carried out in April 2007, May and December 2008, and July 2011 (corresponding to different hydrological regimes of the Rhône River).

These comparisons were based on the information contained in dissimilarity matrices computed using: (1) $D_{0.5}$, POC, Chl-*a*, Phaeo-*a*, Chl-*a*/(Chl-*a*+Phaeo-*a*), THAA, EHAA and EHAA/THAA (i.e., all the surface sediment characteristics measured during both studies), and (2) benthic macrofauna abundances. The sums of squared distances from individual points (i.e., station*sampling date) to their group (i.e., station) centroids were computed for each station (following Anderson, 2001 and Anderson et al., 2008) and used as an indices of intra-station temporal variability after standardization for the number of sampling dates.

3. RESULTS

3.1. WGMP: Water flows and Bottom Shear Stress over the 2010-2018 period

1
2 Water flows presented a clear seasonal pattern with winter floods (peaks up to 5 590
3 $\text{m}^3.\text{s}^{-1}$ on January 23 2018) and low-flow periods during summer and fall (Figure 2A). Over the
4 whole 2010-2018 period, major events were the January 2018 and to a slightly lower extent the
5 January 2014 floods. Between October 2016 and April 2018, there were clear inter-annual
6 differences in water flows during the high-flow period as indicated by the moderate values
7 recorded during the 2016-2017 as opposed to 2017-2018 winter. The July 2010 cruise (Massé
8 et al., 2016) was achieved immediately after the end of a high-flow period. The October 2016
9 and August 2017 cruises were achieved during low-flow periods (112 and 67 days after the end
10 of the preceding high-flow period, respectively). Conversely, both the February 2018 and April
11 2018 cruises took place during a high-flow period, respectively 5 and 87 days after the January
12 2018 flood.

13
14 Although clearly decreasing with depth, Bottom Shear Stress (BSS) showed similar
15 temporal patterns at all 5 stations (Lamarque et al., 2021). Their temporal changes are therefore
16 only presented for station 3. BSS showed a clear seasonal pattern with a succession of peaks
17 induced by winter storms and conversely low values during summer and fall (Figure 2B). Over
18 the whole 2010-2018 period, the major event was the succession of peaks (i.e., up to 3.23 N.m^{-2}
19 2) induced by the repetition of strong storms during the 2013-2014 winter. The July 2010 cruise
20 (Massé et al. 2016) was achieved at the end of a low-BSS period. During the 2016-2018 period,
21 there were slight differences between temporal changes in water flows and BSS since: (1) high-
22 BSS periods generally preceded high-flow periods, and (2) highest BSS (up to 2.40 N.m^{-2} on
23 February 3 2017) were recorded during 2016-2017 *versus* 2018 for highest water flows.
24 Nevertheless, both the October 2016 and August 2017 cruises were conducted during low-BSS
25 periods (i.e., $<0.5 \text{ N.m}^{-2}$) as opposed to the February 2018 and April 2018 cruises, which both
26 took place during the 2017-2018 high-BSS period.

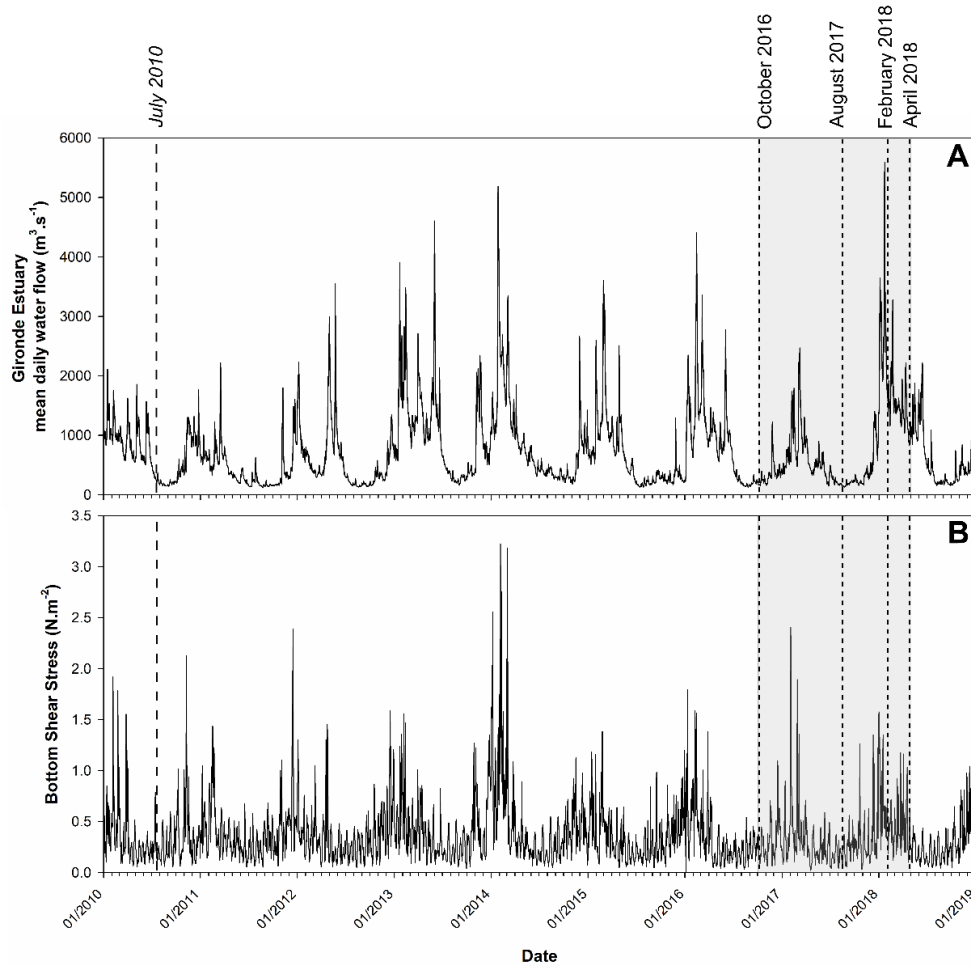


Figure 2. WGMP: Temporal changes in Gironde Estuary mean daily water flows (A) and in the 95th percentile of Bottom Shear Stress at station 3 (B) between 2010 and 2018. Short-dashed lines indicate the 4 cruises achieved in 2016-2018 (grey area) and the long-dashed line indicates the July 2010 cruise (Massé et al., 2016).

3.2. WGMP: 2016-2018 spatiotemporal changes in surface sediment characteristics

$D_{0.5}$ of surface sediments were usually larger (60, 76 and 92 μm in October 2016, August 2017 and February 2018, respectively) and much more variable (16 μm in April 2018) at station 1 (Table II, Figure 3A). At all other stations, $D_{0.5}$ were homogeneous (mean values around 20 μm) and temporally stable. Spatiotemporal changes in $\delta^{13}\text{C}$ were limited (i.e., between -25.12 and -23.01 ‰) with the exception of station 1 in October 2016 (-18.11 ‰, Table II, Figure 3B). Particulate Organic Carbon (POC) clearly increased with station depth (i.e., from stations 1 to 4), with a maximal value of 1.79 mg.m^{-2} of Sediment Surface Area (SSA) at station 4 during April 2018 (Table II, Figure 3C). The only exception to this pattern was February 2018 with a maximal value of 1.58 mg.m^{-2} SSA at station 3. At station 4, POC was higher in April 2018 than during the 3 other cruises (mean value of 1.44 mg.m^{-2} SSA). Total Hydrolysable Amino Acids concentrations (THAA) also increased with station depth

(Table II, Figure 3D). THAA ranged from 0.51 mg.gDW⁻¹ (station 1 in August 2017) to 4.65 mg.gDW⁻¹ (stations 3 and 4 in April 2018). Temporal changes in THAA were lower at station 4 (variation coefficient of 5.4 % *versus* a mean of 22.0 % at the 4 other stations). Chlorophyll-*a* concentrations (Chl-*a*) at station 1 were low (i.e., between 0.23 and 0.66 µg.gDW⁻¹ in August 2017 and April 2018, respectively) during all cruises, (Table II, Figure 3E). At all other stations, Chl-*a* were much higher in April 2018 (with a maximal value of 5.86 µg.gDW⁻¹ at station 4) than during the 3 other cruises (mean value of 1.09 ± 0.37 µg.gDW⁻¹ for stations 2, 3, 8 and 4). The ratio between Enzymatically and Total Hydrolysable Amino Acids (EHAA/THAA) clearly decreased with station depth (Table II, Figure 3F). EHAA/THAA was maximal (41.0 %) at station 1 in February 2018 and minimal (9.1 %) at station 4 in August 2017. Temporal changes were larger at stations 4 and 1 (variation coefficient of 21.0 and 19.2 %, respectively) than at the 3 other stations (mean variation coefficient of 12.7 %).

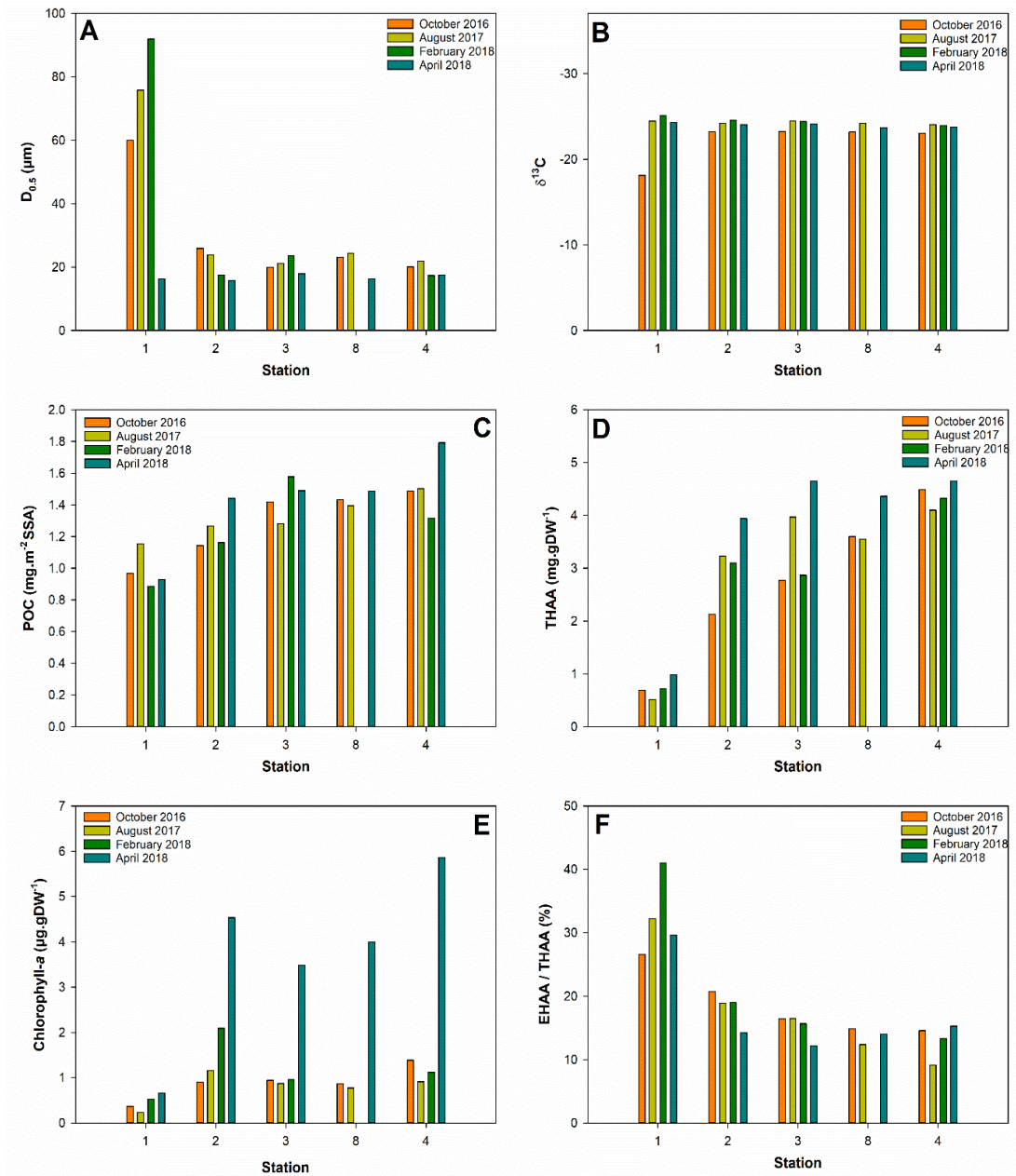


Figure 3. *WGMP*: Spatiotemporal changes in the (mean) values of surface sediment characteristics during the 4 cruises achieved between 2016 and 2018: Median grain sizes ($D_{0.5}$; **A**), $\delta^{13}C$ (**B**), Particulate Organic Carbon concentrations normalized by SSA (POC; **C**), Total Hydrolysable Amino Acids concentration (THAA; **D**), Chlorophyll-*a* concentrations (**E**), and Enzymatically/Total Hydrolysable Amino Acids ratios (EHAA/THAA; **F**). Stations are ordered according to their depth.

The Pearson correlation coefficients linking the similarity matrix based on integrated river flows and those based on either surface sediment characteristics or benthic macrofauna compositions are shown in Figure 4A. When using surface sediment characteristics, correlation coefficients first increased with integration period durations, became significant for a 53-day integration period and reached a maximal value of 0.34 for integration periods between 156

and 222 days. They then decreased constantly down to a value of 0.01 for an integration period of 365 days. When using benthic macrofauna compositions, correlation coefficients remained insignificant over the whole range of river flows integration periods.

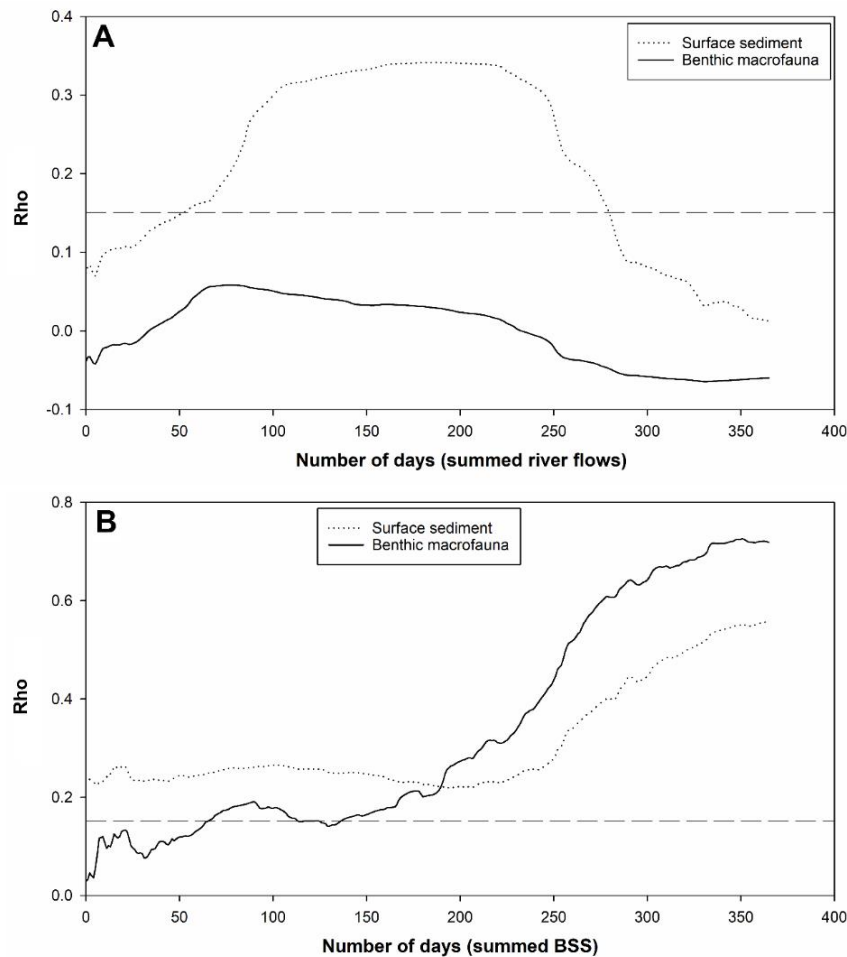


Figure 4. WGMP: Changes in the Pearson correlation coefficient (Rho) linking the similarity matrices based on either surface sediment characteristics or benthic macrofauna compositions (data collected between 2016 and 2018) with river flows (A) and Bottom Shear Stress (B) integrated over 1 to 365-day time periods preceding the 4 cruises. Dotted lines represent 5 % significance thresholds.

The Pearson correlation coefficients linking the similarity matrix based on integrated BSS and those based on either surface sediment characteristics or benthic macrofauna compositions are shown in Figure 4B. In both cases, they increased with BSS integration periods and their maximal values were reached around 1-year (i.e., 0.56 and 0.73 at 365 and 351 days for surface sediment characteristics and benthic macrofauna compositions, respectively). However, the patterns of changes with increasing integration periods clearly differed. When using surface sediment characteristics, correlation coefficients were always significant and almost constant for integration periods between 1 to ca. 250 days. Conversely, when using benthic macrofauna compositions, correlation coefficients were not significant for integration periods shorter than 65 days. They then presented a relative maximum (0.19 for a

90-day integration period) before almost constantly increasing for integration periods longer than 130 days.

The first two components of the PCA based on surface sediment characteristics accounted for 72.8 % (i.e., 55.4 % and 17.4 %, respectively) of their total variance (Figure 5A). Hierarchical clustering and the associated SIMPROF procedure resulted in the identification of 3 groups and 2 “isolated” stations*dates (Figure 5A). “Isolated” stations*dates consisted of station 2 in February 2018 and station 4 in April 2018. Group I was exclusively composed of stations 1 (all sampling dates). Group II was composed of all remaining stations*dates except for the April 2018 cruise. All the stations sampled during this cruise clustered into group III, except stations 1 (Group I) and 4 (isolated). The first principal component was mostly defined by the opposition between the quantitative and qualitative characteristics of surface sedimentary organics with THAA, EHAA, POC, Chl-*a*, Phaeo-*a* and POC concentrations on one side and EHAA/THAA on the other. The second component was mostly defined by the Chl-*a*/(Chl-*a*+Phaeo-*a*) and to a lesser extent EHAA/THAA (Figure 5B).

The DISTLM included river flows and BSS integrated over both 100- and 365-day periods (hereafter Flow₁₀₀, Flow₃₆₅, BSS₁₀₀ and BSS₃₆₅) as independent variables. It explained 70.7 % of the total variance of surface sediment characteristics. Its representation through the first plane of the dbRDA accounted for 61.6 % of this total variance and showed two main orientations (Figure 5C). The first one, mainly along the first component of the dbRDA, corresponded to the positioning of the stations along the depth gradient and was mainly cued by BSS₃₆₅. The second one, mainly along the second component of the dbRDA, separated the 4 cruises and was mainly cued by Flow₁₀₀ and to a lesser extent BSS₁₀₀. Cumulated and Annual Julian Days (CJD and AJD, respectively) correlated significantly ($p < 0.05$) with this second orientation. This correlation was slightly higher for CJD ($r = 0.934$ *versus* $r = 0.822$).

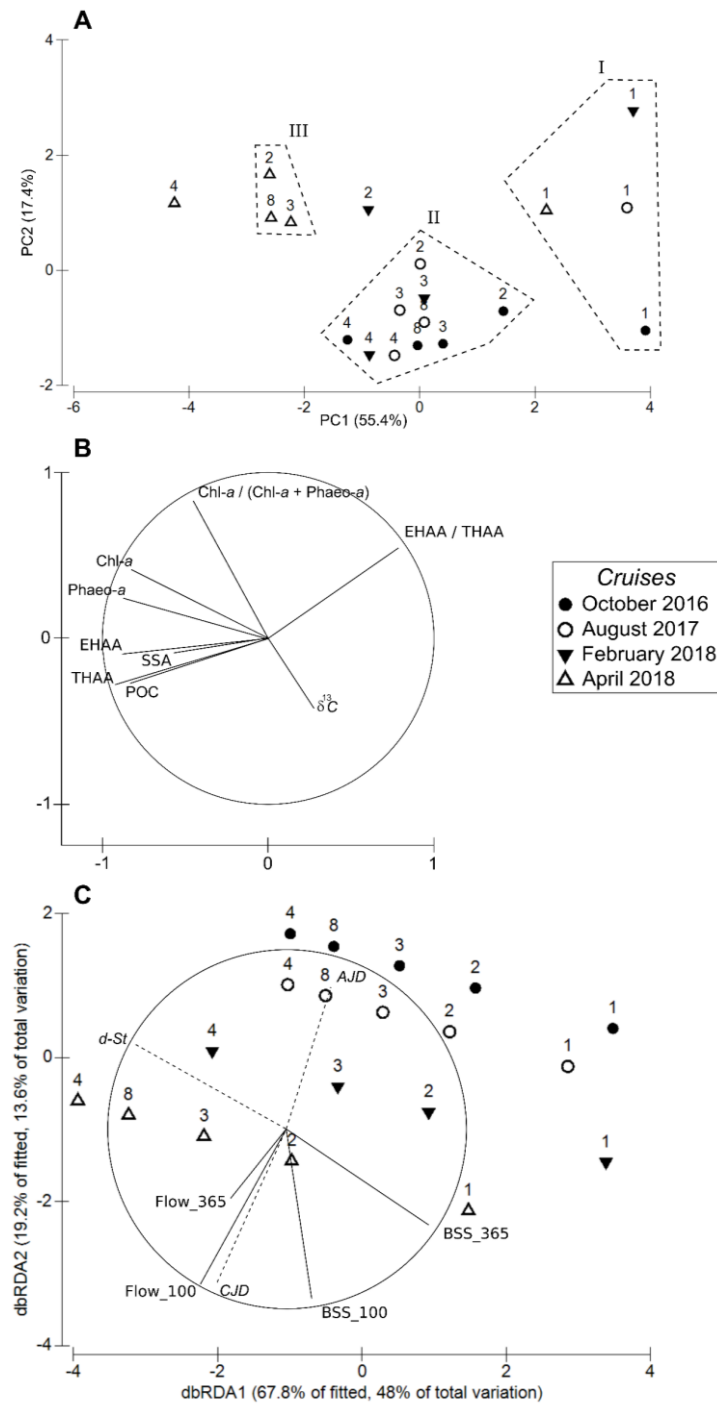


Figure 5. WGMP: Multivariate analyses of surface sediment characteristics recorded between 2016 and 2018. Projection of stations*crises on the first plane of a Principal Component Analysis (A). Figures refer to stations and symbols to cruises. Dotted lines indicate groups of stations*crises issued from hierarchical clustering. Correlations of the variables with the first two principal components (B). Distance-based Redundancy Analysis based on integrated Bottom Shear Stress and river flows (C). Station depth (*d-St*), Annual Julian Days (*AJD*) and Cumulated Julian Days (*CJD*) were used as supplementary variables. SSA: Sediment Surface Area; POC: Particulate Organic Carbon; Chl-*a*: Chlorophyll-*a*; Phaeo-*a*: Phaeophytin-*a*; THAA; Total Hydrolysable Amino Acids; EHAA: Enzymatically Hydrolysable Amino Acids; BSS_100 and BSS_365: integrated Bottom Shear Stress over 100 and 365 days; Flow_100 and Flow_365: integrated river flows over 100 and 365 days. (See text for details)

3.3. WGMP: 2016-2018 spatiotemporal changes in benthic macrofauna compositions

Overall, 6391 specimens belonging to 146 taxa were collected and identified (123 taxa after pooling species at the *Ampelisca*, *Glycera* and *Nephtys* genus). Molluscs (mainly abundant at stations 1 and 2) represented 34 % of total macrofauna abundance, followed by polychaetes (27.8 %), echinoderms (22 %) and crustaceans (13.4 %).

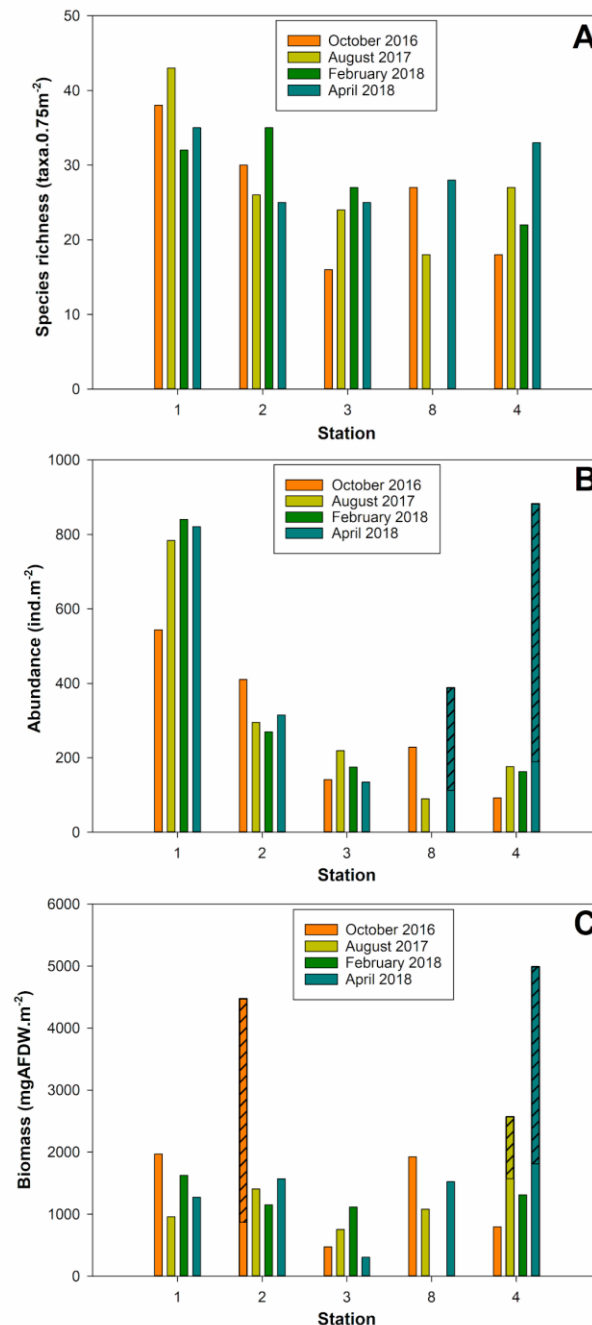


Figure 6. WGMP: Spatiotemporal changes in the (mean) values of main univariate benthic macrofauna characteristics recorded between 2016 and 2018: species richness (A), abundance (B), and biomass (C). Hatching corresponds to the exceptional presence of: (1) numerous individuals of a single taxon for abundance barplot and (2), high biomass of a single taxon for biomass barplot. Stations are ordered according to their depth.

Species richness did not show any clear spatiotemporal pattern (Table II, Figure 6A). It seemed higher at station 1, with a maximum of 43 taxa in August 2017. It tended to decrease from stations 1 to 3, where a minimal value of 16 taxa was recorded in October 2016. Species richness then seemed to increase from stations 3 to 4 in August 2017 and April 2018. Equitability tended to be lower at stations 1 and 2 than at stations 3, 8 and 4 (Table II). It was temporally more stable at stations 1 and 2 than at stations 8 and 4, whose variability resulted from low values in April 2018 caused by the exceptionally high abundances of *Ampelisca spp.* and *Hyala vitrea*. Mean macrobenthic abundances were between 882.7 (station 4*April 2018) and 89.3 (station 8*August 2017) individuals per m² (Table II, Figure 6B). Abundances were higher at station 1 and tended to decrease with station depth. Only stations 8*April 2018 and 4*April 2018 differed from this general pattern with especially high values due to high abundances of *Ampelisca spp.* (182.7 and 593.3 individuals per m² at station 8 and 4 respectively) and *Hyala vitrea* (93.3 and 100.0 individuals per m² at stations 8 and 4 respectively). Changes in mean macrobenthic biomasses did not show any clear spatiotemporal pattern (Table II, Figure 6C) and were characterized by the occurrence of 3 outliers featuring high values. The high biomass recorded for station 2*October 2016 resulted from the presence of both a single individual of *Asterias rubens* (2019.0 mgAFDW) and a high biomass of numerous individuals (i.e., 57.3 per m²) of *Abra alba* (910.6 mgAFDW.m⁻²). The high biomasses recorded for station 4*August 2017 and station 4*April 2018 both resulted from the presence of single individuals of *Cereus pedunculatus* in August 2017 (747.0 mgAFDW) and of *Nephrops norvegicus* in April 2018 (2379.2 mgAFDW).

The nMDS based on 2016-2018 macrofauna abundance data is shown in Figure 7A. The horizontal dimension of the reduced space corresponded to station depth, reflecting the progressive change in benthic macrofauna compositions along this gradient. *Amphiura filiformis* and *Kurtiella bidentata* accounted for 20.6 and 40.9 % of total macrofauna abundance at station 1 (43.4 and 10.3 % at station 2). Stations 8 and 4 were, conversely, characterized by the presence of burrowing macrofauna (e.g. *Callianassa subterranea* and *Oestergrenia digitata*). For all stations, the vertical dimension of the reduced space mostly separated sampling cruises. The dispersion of the different cruises for each station suggests that between-cruises changes in benthic macrofauna compositions were larger at deep (i.e., stations 3, 4 and 8) than at shallow (i.e., stations 1 and 2) stations. The hierarchical clustering further confirmed this pattern with the identification of 5 groups: (I) station 1 in February and April 2018, (II) station 2 during all cruises, (III) station 3 in February and April 2018, (IV) stations 8 and 4 in October 2016, and (V) stations 8 and 4 in August 2017, February 2018 and April 2018.

The DISTLM involving surface sediment characteristics as predictive variables included THAA and Chl-*a*. It explained 42.0 % of the total variance of benthic macrofauna compositions. Its representation through the first plane of the dbRDA also accounted for 42.0 % of this total variance and showed two main orientations (Figure 7B). The first one, mainly along the first component of the dbRDA, corresponded to station depth and was mainly explained by THAA. The second one, mainly along the second component of the dbRDA, separated stations (except station 1) sampled during April 2018 from all other stations*dates, and was mainly cued by Chl-*a* concentrations. CJD correlated significantly with this second orientation ($r = 0.560$, $p < 0.05$) but not AJD ($r = 0.393$, $p = 0.07$). The DISTLM involving

BSS and river flows included BSS₃₆₅, Flow₁₀₀ and Flow₃₆₅ as independent variables. It explained 53.5 % of the total variance of benthic macrofauna compositions. Its representation through the first plane of a dbRDA accounted for 49.9 % of this initial variance and here again showed two main orientations (Figure 7C). The first one, mainly along the first component of the dbRDA, corresponded to station depth and was mainly explained by BSS₃₆₅. The second one, mainly along the second component of the dbRDA, separated the 4 cruises, and was mainly cued by Flow₁₀₀. The contribution of Flow₃₆₅ was poorly described by the first plane of the dbRDA. CJD and AJD correlated significantly ($p < 0.05$) with this second orientation. This correlation was slightly higher for CJD ($r = 0.992$ versus $r = 0.820$).

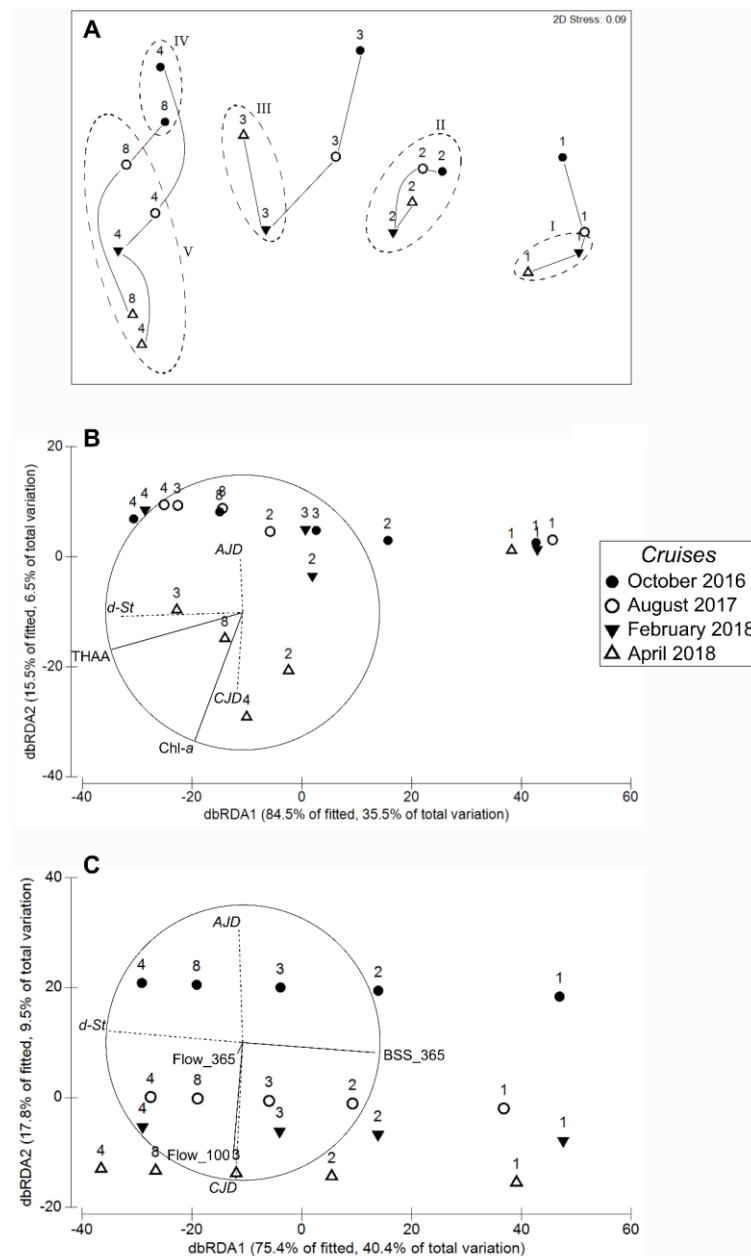


Figure 7. WGMP: Multivariate analyses of spatiotemporal changes in benthic macrofauna compositions recorded between 2016 and 2018. Non-Metric Multidimensional Scaling of benthic macrofauna compositions data for stations*dates during 2016-2018 cruises (A). Figures refer to stations and symbols to cruises. Solid lines represent trajectories of stations

1 over time and dotted lines indicate groups of stations*dates issued from hierarchical clustering.
2 Distance-based Redundancy Analysis based on surface sediment characteristics (**B**). Distance-
3 based Redundancy Analysis based on integrated BSS and river flows (**C**). Station depth (*d-St*),
4 Annual Julian Days (*AJD*) and Cumulated Julian Days (*CJD*) were used as supplementary
5 variables. Chl-*a*: Chlorophyll-*a*; THAA; Total Hydrolysable Amino Acids; BSS_365:
6 integrated Bottom Shear Stress over 365 days; Flow_100 and Flow_365: integrated river flows
7 over 100 and 365 days.

1 **Table II.** *WGMP*: Mean values (\pm standard deviations for replicated measures) of surface sediment and main univariate benthic macrofauna
2 characteristics during the 4 cruises achieved between 2016 and 2018. $D_{0.5}$: median grain size, SSA: Sediment Surface Area, POC: Particulate
3 Organic Carbon, Chl-*a*: Chlorophyll-*a*, Phaeo-*a*: Phaeophytin-*a*, THAA: Total Hydrolyzable Amino Acids, EHAA: Enzymatically Hydrolyzable
4 Amino Acids, SR: Species Richness and J' : Pielou's evenness.

Cruise	Station	$D_{0.5}$ (μm)	SSA ($\text{m}^2\cdot\text{gDW}^{-1}$)	POC ($\text{mg}\cdot\text{m}^{-2}$ SSA)	Chl- <i>a</i> ($\mu\text{g}\cdot\text{gDW}^{-1}$)	Phaeo- <i>a</i> ($\mu\text{g}\cdot\text{gDW}^{-1}$)	Chl- <i>a</i> /(Chl- <i>a</i> +Phaeo- <i>a</i>) (%)	THAA ($\text{mg}\cdot\text{gDW}^{-1}$)	EHAA ($\text{mg}\cdot\text{gDW}^{-1}$)	EHAA/THAA (%)	$\delta^{13}\text{C}$ (‰)	Abundance ($\text{ind}\cdot\text{m}^{-2}$)	Biomass ($\text{mgAFDW}\cdot\text{m}^{-2}$)	SR ($\text{taxa}\cdot 0.75\text{m}^{-2}$)	J'
October 2016	1	60.0	5.0	0.97	0.36 ± 0.10	2.95 ± 0.27	10.9 ± 2.0	0.69 ± 0.06	0.18 ± 0.05	26.5 ± 4.5	-18.11 ± 0.41	544.0 ± 198.9	1969.2 ± 2260.5	38	0.73
	2	26.0	6.1	1.14	0.90 ± 0.36	8.27 ± 1.05	10.0 ± 4.6	2.13 ± 0.13	0.44 ± 0.06	20.7 ± 1.8	-23.20 ± 0.05	410.7 ± 112.0	4473.4 ± 4494.1	30	0.69
	3	20.0	8.1	1.42	0.94 ± 0.02	8.39 ± 1.11	10.2 ± 1.3	2.77 ± 0.10	0.45 ± 0.02	16.4 ± 1.1	-23.23 ± 0.13	141.3 ± 68.2	474.2 ± 433.1	16	0.89
	8	23.1	7.5	1.43	0.87 ± 0.35	6.75 ± 0.37	11.3 ± 4.2	3.60 ± 0.23	0.53 ± 0.07	14.9 ± 2.6	-23.16 ± 0.08	228.0 ± 28.0	1922.4 ± 890.6	27	0.88
	4	20.1	10.3	1.49	1.39 ± 0.47	9.59 ± 1.69	13.0 ± 5.8	4.49 ± 0.27	0.65 ± 0.12	14.6 ± 3.2	-23.01 ± 0.03	92.0 ± 42.3	796.2 ± 418.2	18	0.92
August 2017	1	75.8	2.5	1.15	0.23 ± 0.09	1.46 ± 0.46	13.4 ± 2.5	0.51 ± 0.18	0.16 ± 0.04	32.2 ± 3.8	-24.44 ± 0.35	784.0 ± 360.6	958.1 ± 552.5	43	0.67
	2	23.8	7.3	1.27	1.15 ± 0.20	6.65 ± 0.88	14.9 ± 2.7	3.23 ± 0.29	0.61 ± 0.02	18.9 ± 1.4	-24.22 ± 0.55	294.7 ± 109.3	1405.8 ± 259.1	26	0.68
	3	21.2	8.4	1.28	0.87 ± 0.05	6.07 ± 1.64	13.1 ± 3.2	3.97 ± 0.07	0.66 ± 0.10	16.5 ± 2.2	-24.46 ± 0.10	218.7 ± 154.6	754.9 ± 189.9	24	0.67
	8	24.4	7.6	1.40	0.77 ± 0.29	5.25 ± 0.57	12.7 ± 4.0	3.55 ± 0.10	0.44 ± 0.01	12.3 ± 0.5	-24.22 ± 0.19	89.3 ± 43.1	1081.0 ± 1147.4	18	0.92
	4	21.9	9.3	1.50	0.91 ± 0.18	6.90 ± 1.28	12.0 ± 4.0	4.10 ± 0.19	0.38 ± 0.02	9.1 ± 0.5	-24.03 ± 0.38	176.0 ± 60.4	2569.4 ± 1698.6	27	0.92
February 2018	1	92.0	1.9	0.89	0.52 ± 0.37	2.53 ± 1.58	16.4 ± 1.8	0.72 ± 0.32	0.29 ± 0.12	41.0 ± 2.0	-25.12 ± 0.23	840.0 ± 342.0	1625.4 ± 541.0	32	0.62
	2	17.5	14.2	1.16	2.09 ± 0.72	9.61 ± 2.47	17.6 ± 1.5	3.10 ± 0.16	0.59 ± 0.14	19.0 ± 4.2	-24.58 ± 0.48	269.3 ± 217.0	1149.6 ± 1093.7	35	0.81
	3	23.7	6.2	1.58	0.96 ± 0.19	6.22 ± 0.63	13.3 ± 1.3	2.87 ± 0.43	0.45 ± 0.06	15.7 ± 0.3	-24.41 ± 0.01	174.7 ± 130.1	1113.3 ± 1190.6	27	0.85
	4	17.4	12.6	1.32	1.12 ± 0.17	9.51 ± 1.86	10.6 ± 1.0	4.32 ± 0.43	0.57 ± 0.07	13.3 ± 3.0	-23.91 ± 0.10	162.7 ± 112.4	1313.4 ± 1035.7	22	0.88
April 2018	1	16.3	12.9	0.93	0.66 ± 0.05	3.67 ± 0.38	15.2 ± 0.5	0.98 ± 0.51	0.26 ± 0.04	29.6 ± 11.0	-24.29 ± 0.002	821.3 ± 615.5	1271.2 ± 175.0	35	0.62
	2	15.8	11.0	1.44	4.54 ± 1.96	18.16 ± 8.17	20.1 ± 0.6	3.94 ± 0.67	0.56 ± 0.07	14.2 ± 1.4	-24.05 ± 0.05	314.7 ± 32.6	1569.5 ± 1071.7	25	0.67
	3	17.9	7.7	1.49	3.48 ± 1.98	15.57 ± 8.18	18.1 ± 0.6	4.65 ± 1.44	0.56 ± 0.11	12.2 ± 1.2	-24.11 ± 0.20	134.7 ± 50.0	306.8 ± 354.9	25	0.84
	8	16.2	10.0	1.48	3.99 ± 1.66	18.37 ± 6.26	17.6 ± 2.1	4.36 ± 0.26	0.61 ± 0.03	14.0 ± 0.9	-23.69 ± 0.18	388.0 ± 69.4	1522.5 ± 1301.5	28	0.62
	4	17.4	8.9	1.79	5.86 ± 0.85	29.35 ± 2.83	16.6 ± 1.3	4.65 ± 0.49	0.72 ± 0.20	15.3 ± 2.8	-23.74 ± 0.31	882.7 ± 202.6	4985.9 ± 5475.4	33	0.45

3.4. WGMP: 2010/2016-2018 spatiotemporal changes in benthic macrofauna compositions

The 2010/2016-2018 comparison of univariate benthic macrofauna descriptors highlighted major differences between July 2010 (Massé et al., 2016) and the 2016-2018 cruises. Species richness values were in the same order of magnitude in July 2010 (32, 22 and 21 taxa at stations 1, 3 and 4, respectively) and in 2016-2018 (means of 37, 23 and 25 taxa at stations 1, 3 and 4, respectively). Conversely, abundances were much higher at station 1 in July 2010 than during all 2016-2018 cruises (1628.0 vs 747.3 ± 137.5 ind.m⁻², respectively). Abundances were also higher at station 3 in July 2010 (328.0 vs 167.4 ± 38.5 ind.m⁻²). They conversely tended to be equivalent at station 4 (118.7 in July 2010 vs 155.0 ± 43.4 ind.m⁻² during 2016-2018 cruises) when excluding the numerous *Ampelisca* spp. and *Hyala vitrea* individuals present in April 2018. Biomasses were higher at stations 1 and 3 in July 2010 (4696.0 and 3495.7 mgAFDW.m⁻², respectively) than during the 2016-2018 cruises (means of 1456.0 ± 437.5 and 662.3 ± 353.0 mgAFDW.m⁻², respectively). They also tended to be equivalent at station 4 between July 2010 (1901.9 mgAFDW.m⁻²) and 2016-2018 cruises (1374.2 ± 436.1 mgAFDW.m⁻²) when excluding the large and rarely present individuals identified at station 4 during August 2017 and April 2018 (see section 3.3).

The representation of stations*dates through the nMDS based on macrofauna abundance data from the 2010 and 2016-2018 cruises is shown in Figure 8. The horizontal dimension accounted for the positioning of stations along the depth gradient, whereas the vertical dimension separated sampling dates and more specifically July 2010 (Massé et al., 2016) from all the 2016-2018 cruises. Hierarchical clustering confirmed this pattern with the identification of 5 clusters. The first 4 were almost identical to those of the analysis conducted on the sole 2016-2018 data (see above) and group V was only constituted by stations 3 and 4 in July 2010. The positioning of stations*dates along the horizontal dimension were similar in 2010 and 2016-2018 as opposed to their positioning along the second dimension, which showed major 2010/2016-2018 changes in benthic macrofauna compositions and suggested that these changes were larger at stations 3 and 4 than at station 1.

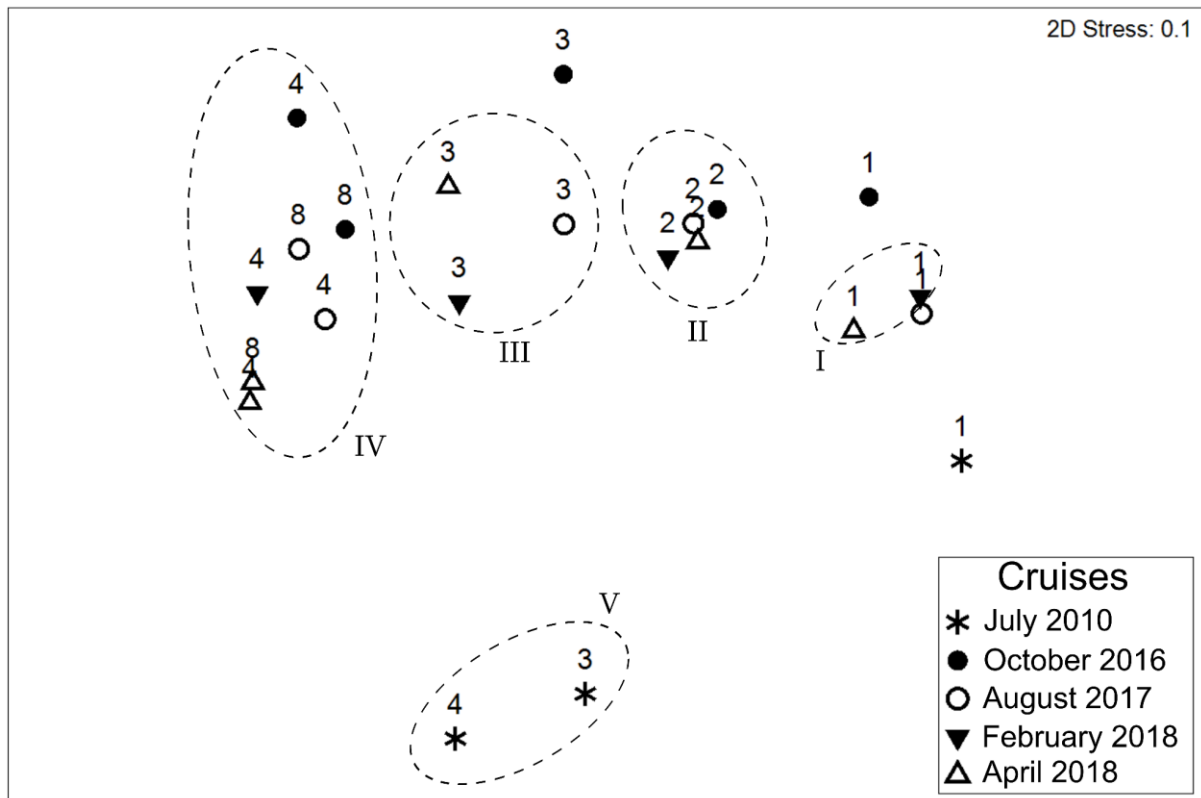


Figure 8: WGMP: non-Metric Multidimensional Scaling of 2010/2016-2018 spatiotemporal changes in benthic macrofauna compositions. Data for stations*dates have been collected during both the 2010 and 2016-2018 cruises. Figures refer to stations and symbols to cruises. Dotted lines indicate the groups of samples issued from hierarchical clustering.

3.5. Comparison of spatiotemporal changes in surface sediment characteristics and benthic macrofauna compositions within the WGMP and the RRP

The relationships between station depth and intra-station temporal variabilities in surface sediment characteristics (Figure 9A) and benthic macrofauna compositions (Figure 9B) both largely differed in the West Gironde Mud Patch (WGMP) and the Rhône River Prodelta (RRP). In both cases, and although caution should clearly be taken when comparing absolute values of WGMP and RRP data, highest intra-station variabilities were associated with the RRP shallowest station. Intra-station temporal variabilities in RRP surface sediment characteristics decreased with station depth. Conversely, they did not show any clear pattern relative to station depth in the WGMP. In the RRP temporal variabilities in benthic macrofauna compositions was much higher at the shallowest station (i.e., station A) than at the 4 other stations, whereas in the WGMP, they were lower at the two shallowest stations.

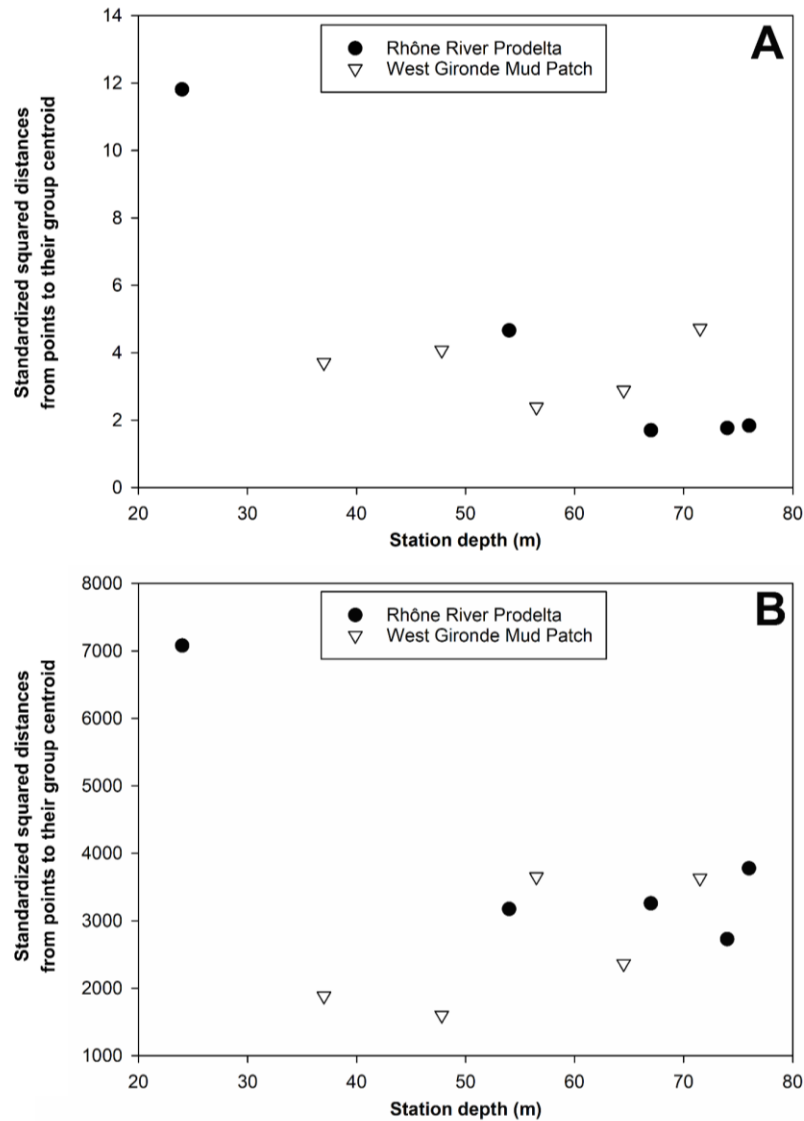


Figure 9. Comparison between the West Gironde Mud Patch (WGMP) and the Rhône River Prodelta (RRP): Relationship between station depth and intra-station temporal variabilities (standardized squared distances from points to their group centroid) in sediment surface characteristics (A) and benthic macrofauna compositions (B) in both the WGMP (data collected between 2016 and 2018) and the RRP (data collected between 2007 and 2011; Bonifácio et al., 2014). (See text for details)

4. DISCUSSION

4.1. WGMP 2016-2018 spatiotemporal changes

4.1.1. Surface sediment characteristics

Spatial changes in surface sediment characteristics were larger than temporal ones. Station 1 was located in the proximal part of the West Gironde Mud Patch (WGMP). It presented coarser surface sediments during 3 cruises (i.e., October 2016, August 2017 and February 2018) than during April 2018. This likely resulted from the transient deposition of coarser sediments during high-energy events (Lesueur et al., 1991, 1996, 2001, 2002; Lesueur and Tastet, 1994). All other 4 stations were located in the distal part. They presented restricted spatial changes in surface sediment granulometry, but conversely a clear increase in bulk organic contents (i.e., Particulate Organic Carbon and Total Hydrolysable Amino Acids) with station depth, which supports previous observations by Lamarque et al. (2021) and Massé et al. (2016). Such a pattern is rather uncommon in River-dominated Ocean Margins (RiOMar; e.g., Bonifacio et al., 2014; Cathalot et al., 2013; Goñi et al., 1998; Gordon et al., 2001; Keil et al., 1997) and has been attributed to a particle sieving process cued by particle density (Lamarque et al., 2021) rather than size (Hedges and Keil, 1995; Keil et al., 1998; Mayer, 1994a, b) during the succession of sedimentation/resuspension cycles governing the transfer of particles offshore in RiOMar (Blair and Aller, 2012). The results of the DISTLM/dbRDA analysis support the predominant role of local hydrodynamics as the driving factor of the spatial distribution of surface sediment characteristics in the WGMP as already put forward by Lamarque et al. (2021) based on a synoptic spatial survey. Caution should nevertheless be taken in interpreting this result since river flows did not include any spatial component.

The importance of the seasonal component in driving 2016-2018 temporal changes in surface sediment characteristics is supported by the results of the DISTLM/dbRDA analysis, showing that temporal changes correlate better with river flows, and to a lesser extent hydrodynamics, integrated over a seasonal (i.e., Flow₁₀₀ and BSS₁₀₀) than a yearly period (i.e., Flow₃₆₅ and BSS₃₆₅). The most important changes in surface sediment characteristics occurred during spring 2018. A spring increase in chloropigment concentrations has already been reported by Relexans et al. (1992) in the distal part of the WGMP. The seasonality of pelagic primary production in this area of the Bay of Biscay is characterized by the occurrence of a spring phytoplankton bloom (Herbland et al., 1998; Labry et al., 2002). Both fluorescence profiles and satellite image analyses (Copernicus Sentinel data 2018 processed using SNAP software, data available on request to B. Lamarque) confirmed that the period immediately preceding April 2018 was characterized by high Chlorophyll-*a* (Chl-*a*) concentrations (i.e., ca. 10 mg.m⁻³) in surface waters overlying the WGMP. The high chloropigment concentrations and Chl-*a*/(Chl-*a*+Phaeo-*a*) recorded in surface sediments during April 2018 thus probably resulted from the sedimentation of a spring bloom.

4.1.2. Benthic macrofauna

Our results clearly show the higher importance of spatial relative to 2016-2018 temporal changes in benthic macrofauna composition. Benthic macrofauna compositions changed with station depth. The spatial pattern observed in July 2010 by Massé et al. (2016) was strongly dominated by differences between the proximal (i.e., station 1) and the distal (i.e.,

stations 3 and 4) parts. During the present study, stations 1 and 2 were dominated by *Amphiura filiformis* and *Kurtiella bidentata*, which is consistent with the presence of the *A. filiformis*-*K. bidentata*-*Abra nitida* community in cohesive muddy sands off wave exposed coast (Hiscock, 1984; Picton et al., 1994). This corresponds to the A5.351 (“*Amphiura filiformis*, *Kurtiella bidentata* and *Abra nitida* in circalittoral sandy mud”) habitat of the EUNIS classification (Bajjouk et al., 2015). Stations 8 and 4 were strongly bioturbated (Lamarque et al., 2021 and unpubl. data) and characterized by the presence of: (1) a large variety of polychaetes, (2) seapens (*Cavernularia pusilla* and *Veretillum cynomorium*) and (3) *Nephrops norvegicus* (G. Bernard, personal observation). They therefore can be related with the EUNIS A5.361 (“Seapens and burrowing megafauna in circalittoral fine mud”) habitat (Bajjouk et al., 2015). Our results thus confirm that benthic macrofauna compositions clearly differ between the proximal and distal parts of the WGMP. They however also show the occurrence of a depth gradient in these compositions within the sole distal part.

Overall, benthic macrofauna abundances tended to decrease with depth, which is conform to the trend observed by Massé et al. (2016). Such a decreasing pattern is not fully consistent with the results of surveys achieved in other RiOMar, where increasing trends in benthic macrofauna abundances with the distance to the river mouth have been most often observed (Akoumianaki et al., 2013; Aller and Aller, 1986; Alongi et al., 1992; Bonifácio et al., 2014; Rhoads et al., 1985) and interpreted based on the Rhoads et al. (1985) model. According to this model, benthic macrofauna communities at the immediate vicinity of river mouths are limited by the sediment instability induced by riverine inputs. During the present study, spatial changes in benthic macrofauna compositions correlated best with BSS₃₆₅ and not significantly with river flows. Although caution should clearly be taken (see above), this suggests that local hydrodynamics is the main factor explaining benthic macrofauna composition in the WGMP. Its predominance over riverine inputs within the proximal part being further supported by the lack of modern sedimentation (Lesueur et al., 2002, 2001; Lesueur and Tastet, 1994). Along the same line, the importance of local hydrodynamics in explaining spatial changes in sediment profile image characteristics was put forward by Lamarque et al. (2021). According to the current RiOMar typology (Blair and Aller, 2012), the WGMP would therefore correspond to a type 2/high energy “bypassed” (*sensu* McKee et al., 2004) system where the impact of local hydrodynamics is dominant relative to the one of riverine inputs.

2016-2018 temporal changes in benthic macrofauna compositions tended to be larger at deep stations than at the two shallowest ones, with some evidence that these changes included both a seasonal and an inter-annual component. There are several rationales for the occurrence of seasonal changes. First, in the reduced space of the nMDS, individual station trajectories tended to “close” when they were defined based on Annual Julian Days (AJD), which can be considered as indicative of within year/seasonal variability. Second, temporal changes correlated best with Flow₁₀₀, which suggests the link between changes in seasonally integrated river flows and benthic macrofauna compositions. Third, AJD correlated significantly with the second component of the dbRDA, which was indicative of temporal changes. There is some indirect evidence for an inter-annual component to 2016-2018 temporal changes as well since:

(1) a common inter-annual trend was observed at stations 1, 8 and 4, and (2) the second component of the dbRDA correlated slightly better with Cumulated Julian Days (CJD; indicative of inter-annual/cumulated changes) than with AJD.

4.2. WGMP: 2010/2016-2018 comparison of benthic macrofauna compositions

The existence of an inter-annual component to temporal changes in benthic macrofauna compositions became even more obvious when July 2010 (Massé et al., 2016) and 2016-2018 data were compared. Differences between 2010 and 2016-2018 were indeed much larger than differences observed during 2016-2018. At all 3 sampled stations, differences in benthic macrofauna compositions relative to July 2010 were maximal in October 2016 and, for most of them, changes occurring during the 2016-2018 period tended to reduce those differences, which would be indicative of an ongoing cicatrization process following a major disturbance (Pearson and Rosenberg, 1978) that would have taken place between July 2010 and October 2016.

In the WGMP, local hydrodynamics is a key factor structuring the spatial distributions of benthic macrofauna composition and activity (Lamarque et al., 2021 and above). The frequency of sediment disturbances induced by strong hydrodynamic events have been documented based on the analysis of vertical erosional sequences within the sediment column (Lesueur et al., 2002, 1991; Lesueur and Tastet, 1994). It has been estimated that such disturbances occur every ca. 22 years at 35m depth and only every ca. 80 years at 64m depth (Lesueur et al., 2002). The analysis of the 2010-2018 Bottom Shear Stress time series showed higher values during the 2013-2014 winter when the WGMP experienced higher significant wave heights and a longer total storm duration (i.e., 40 and 300 %, respectively) than the overall means of the 1948-2015 period. Overall, the 2013-2014 winter has been the most energetic during the 1948-2015 period along most of the European Atlantic coast (Masselink et al., 2016). Storm-induced physical disturbance during this uncommon winter is likely to have affected surface sediments, and also possibly, benthic macrofauna compositions over the whole WGMP. In this context, the increase in 2010/2016-2018 temporal changes in benthic macrofauna compositions with station depth may seem counter-intuitive since the intensity of physical disturbance during strong storms is clearly higher at shallower stations. In “normal” conditions (i.e., not during extreme events), these stations are, however, also experiencing tougher hydrodynamics. Moreover, the frequency of extreme events affecting the sediment column and thus potentially benthic macrofauna compositions (Dobbs and Vozarik, 1983; Glémarec, 1978; Rees et al., 1977) also decreases with station depth (Lesueur et al., 2002). One can thus assume that resident benthic macrofauna in the WGMP are less tolerant to physical disturbance at deeper than at shallower stations, thereby accounting for larger changes in benthic macrofauna composition at deeper stations. Based on these elements, our current interpretation is that: (1) the repetition of major storms during the 2013-2014 winter has induced strong physical disturbances of benthic habitats and consequently strong changes in benthic macrofauna compositions over the whole WGMP, and (2) since then temporal changes in benthic macrofauna compositions consist in an ongoing (pluri-annual) cicatrization process

superimposed to a seasonal dynamics (Cárcamo et al., 2017). It should nevertheless be stressed that this working hypothesis clearly remains to be further tested through an extension of the WGMP observation period.

4.3. Comparison between the WGMP and the RRP

Intra-station temporal variabilities in surface sediment characteristics were much higher at the immediate vicinity of the Rhone River Mouth than in the proximal area of the WGMP. In the shallowest area of the Rhône River Prodelta (RRP), this variability is mainly resulting from high sedimentation during floods (Bonifácio et al., 2014; Cathalot et al., 2010; Pastor et al., 2018). Mostly during autumn and winter, part of deposited sediments are resuspended initiating a series of resuspension/depositions, which results in the displacement of fine particles offshore (Marion et al., 2010; Ulses et al., 2008). During this transfer, particles are sorted relative to their size and the most labile particulate organic matter component is degraded (Bonifácio et al., 2014), which contributes to reduce temporal variabilities in surface sediment characteristics in deeper areas. Conversely, temporal variabilities in surface sediment characteristics tended to be constant all over the WGMP. In the proximal part, temporal variability is mostly linked to granulometry, whereas in the distal part, it mostly resulted from elevated chloropigment concentrations and ratios in April 2018. Dilution/mixing effects between continental and marine Particulate Organic Matter sources are affecting the whole WGMP as indicated by the almost constancy in surface sediment $\delta^{13}\text{C}$ and previous water column observations by Fontugne and Jouanneau (1987). Conversely, they clearly increase with the distance to the river mouth (and thus station depth) in the RRP (Bourgeois et al., 2011; Cathalot et al., 2013; Lansard et al., 2009; Tesi et al., 2007). Moreover, due to strong local hydrodynamics, the fine particles originating from the Gironde Estuary do not settle in the proximal part of the WGMP (Lesueur et al., 2001), whereas conversely, high sedimentation rates are taking place at the immediate vicinity of the Rhône River Mouth (Miralles et al., 2005; Zuo et al., 1991). Overall, in the proximal part of the WGMP, this contributes to reduce temporal variabilities in surface sediment characteristics possibly induced by seasonal changes in the hydrological regime of the Gironde Estuary.

Intra-station temporal variabilities in benthic macrofauna compositions showed opposite spatial patterns in the RRP and the WGMP. In the RRP, temporal variabilities were much higher at the immediate vicinity of the Rhône River due to the shift between high and low sedimentation rates during high- and low-flow periods, respectively (Bonifácio et al., 2014). This pattern largely conforms to the Rhoads et al. (1985) model, which attributes a major role to sedimentation in controlling benthic macrofauna in RiOMar. Conversely, temporal variabilities in benthic macrofauna compositions within the WGMP tended to be lower at the 2 shallowest stations than at the 3 deepest ones, which could be attributed a better tolerance of benthic macrofauna to wave-induced disturbance in the shallowest part of the WGMP (see above). Here again, this pinpoints to differences in the relative roles of riverine inputs and local hydrodynamics in explaining spatiotemporal changes within the two systems and thereby supports the current RiOMar typologies (Blair and Aller, 2012; McKee et al., 2004).

5. CONCLUSIONS

The present assessment of 2016-2018 spatiotemporal changes in West Gironde Mud Patch (WGMP) surface sediment characteristics confirms the existence of: (1) a spatial structuration relative to station depth mainly explained by local hydrodynamics, and (2) seasonal changes mainly resulting from the sedimentation of the spring bloom.

Our results also demonstrate the existence of: (1) differences in benthic macrofauna composition between the proximal and distal parts of the WGMP, and (2) a depth gradient in its distal part. Overall, spatial changes in benthic macrofauna composition were best explained by local hydrodynamics integrated over a 1-year period. Benthic macrofauna compositions presented inter-annual changes superimposed over seasonal ones. The marked shift observed between 2010 and 2016-2018 suggests that a major disturbance occurred between these two periods. Our current working hypothesis is that this disturbance was caused by the series of extremely severe winter storms that took place during 2013-2014.

The comparison between the WGMP and Rhône River Prodelta (RRP) shows major differences in the control of temporal variabilities in both surface sediment characteristics and benthic macrofauna compositions within their proximal parts. In the RRP, these variabilities are associated with changes in sedimentation rates in relation with the Rhône River hydrological regime, whereas in the WGMP they result from transient particle deposition induced by intense hydrodynamic events.

Our results further support the characterization of the WGMP as temperate type 2 (i.e., high-energy system) RiOMar. They highlight the different mechanisms involved in the control of surface sediment characteristics and benthic macrofauna compositions in the WGMP and the RRP and are in line with current RiOMar typologies derived from meta-analyses mainly achieved on tropical and subtropical systems (Blair and Aller, 2012; McKee et al., 2004).

Author Contributions: Conceptualization, B.L., B.D., and A.G.; Data curation, B.L.; Formal analysis, B.L. and A.G.; Funding acquisition, B.D. and A.G.; Investigation, B.L., B.D., S.S., G.B., N.D., and A.G.; Methodology, B.L., B.D., S.S., M.D. (Mélanie Diaz), F.G. (Florent Grasso), A.S. and A.G.; Resources, B.L., B.D., S.S., G.B., N.D., M.D. (Mélanie Diaz), N.L., F.G. (Frédéric Garabetian), F.G. (Florent Grasso), A.S., S.R., A.R.-R., M.-A.C., D.P. and M.D. (Martin Danilo); Validation, B.L., B.D., and A.G.; Visualization, B.L. and A.G.; Writing—original draft, B.L. and A.G.; Writing—review and editing, B.L., B.D., S.S., G.B., N.D., F.G. (Frédéric Garabetian), F.G. (Florent Grasso), S.R., A.R.-R. and A.G. All authors have read and agreed to the published version of the manuscript.

Acknowledgements

This work is part of the PhD thesis of Bastien Lamarque (Bordeaux University). Bastien Lamarque was partly supported by a doctoral grant from the French “Ministère de l’Enseignement Supérieur, de la Recherche et de l’Innovation”. This work was supported by: (1) the JERICO-NEXT project (European Union’s Horizon 2020 Research and Innovation program under grant agreement no. 654410), (2) the VOG project (LEFE-CYBER and EC2CO-PNEC), and (3) the MAGMA project (COTE cluster of Excellence ANR-10-LABX-45). It also benefited from additional fundings allocated by the Conseil Régional Nouvelle-Aquitaine and the Office Français de la Biodiversité. Operations at sea were funded by the French Oceanographic Fleet. The authors wish to thank the crew of the R/V Côtes de la Manche for their help during field sampling, Christophe Fontanier, Marie Claire Perello, Pascal Lebleu and Hervé Derriennic for their help during sampling and analyses.

References

- Akaike, H., 1973. Information theory as an extension of the maximum likelihood principle, in: Csaki, F., Petrov, B.N. (Eds.), *Proceedings, 2nd International Symposium on Information Theory*. Budapest, pp. 267–281.
- Akoumianaki, I., Papaspyrou, S., Kormas, K.A., Nicolaidou, A., 2013. Environmental variation and macrofauna response in a coastal area influenced by land runoff. *Estuar. Coast. Shelf Sci.* 132, 34–44. <https://doi.org/10.1016/j.ecss.2012.04.009>
- Aller, J.Y., Aller, R.C., 1986. General characteristics of benthic faunas on the Amazon inner continental shelf with comparison to the shelf off the Changjiang River, East China Sea. *Cont. Shelf Res.* 6, 291–310. [https://doi.org/10.1016/0278-4343\(86\)90065-8](https://doi.org/10.1016/0278-4343(86)90065-8)
- Aller, J.Y., Stupakoff, I., 1996. The distribution and seasonal characteristics of benthic communities on the Amazon shelf as indicators of physical processes. *Cont. Shelf Res.* 16, 717–751. [https://doi.org/10.1016/0278-4343\(96\)88778-4](https://doi.org/10.1016/0278-4343(96)88778-4)
- Aller, R.C., 1998. Mobile deltaic and continental shelf muds as suboxic, fluidized bed reactors. *Mar. Chem.* 61, 143–155. [https://doi.org/10.1016/S0304-4203\(98\)00024-3](https://doi.org/10.1016/S0304-4203(98)00024-3)
- Alongi, D.M., Christoffersen, P., Tirendi, F., Robertson, A.I., 1992. The influence of freshwater and material export on sedimentary facies and benthic processes within the Fly Delta and adjacent Gulf of Papua (Papua New Guinea). *Cont. Shelf Res.* 12, 287–326. [https://doi.org/10.1016/0278-4343\(92\)90033-G](https://doi.org/10.1016/0278-4343(92)90033-G)
- Anderson, M., Gorley, R.N., Clarke, K.R., 2008. *PERMANOVA + for PRIMER user manual*.
- Anderson, M.J., 2001. A new method for non-parametric multivariate analysis of variance. *Austral Ecol.* 26, 32–46. <https://doi.org/https://doi.org/10.1111/j.1442-9993.2001.01070.pp.x>
- Bajjouk, T., Guillaumont, B., Michez, N., Thouin, B., Croguennec, C., Populus, J., Louvel-Glaser, J., Gaudillat, V., Chevalier, C., Tourolle, J., Hamon, D., 2015. Classification EUNIS, Système d’information européen sur la nature : Traduction française des habitats benthiques des Régions Atlantique et Méditerranée. Vol. 2. Habitats subtidaux & complexes d’habitats. <https://doi.org/https://archimer.ifremer.fr/doc/00271/38223/>

- 1 Bischl, B., Lang, M., Bossek, J., Horn, D., Richter, J., Surmann, D., 2017. BBmisc:
2 Miscellaneous Helper Functions for B. Bischl. R Packag. version 1-1-1.
- 3 Blair, N.E., Aller, R.C., 2012. The Fate of Terrestrial Organic Carbon in the Marine
4 Environment. *Ann. Rev. Mar. Sci.* 4, 401–423. [https://doi.org/10.1146/annurev-marine-](https://doi.org/10.1146/annurev-marine-120709-142717)
5 [120709-142717](https://doi.org/10.1146/annurev-marine-120709-142717)
- 6 Bonifácio, P., Bourgeois, S., Labrune, C., Amouroux, J.M., Escoubeyrou, K., Buscail, R.,
7 Romero-Ramirez, A., Lantoiné, F., Vétion, G., Bichon, S., Desmalades, M., Rivière, B.,
8 Deflandre, B., Grémare, A., 2014. Spatiotemporal changes in surface sediment
9 characteristics and benthic macrofauna composition off the Rhône River in relation to its
10 hydrological regime. *Estuar. Coast. Shelf Sci.* 151, 196–209.
11 <https://doi.org/10.1016/j.ecss.2014.10.011>
- 12 Bourgeois, S., Pruski, A.M., Sun, M.Y., Buscail, R., Lantoiné, F., Kerhervé, P., Vétion, G.,
13 Rivière, B., Charles, F., 2011. Distribution and lability of land-derived organic matter in
14 the surface sediments of the Rhône prodelta and the adjacent shelf (Mediterranean Sea,
15 France): A multi proxy study. *Biogeosciences* 8, 3107–3125. [https://doi.org/10.5194/bg-](https://doi.org/10.5194/bg-8-3107-2011)
16 [8-3107-2011](https://doi.org/10.5194/bg-8-3107-2011)
- 17 Burdige, D.J., 2005. Burial of terrestrial organic matter in marine sediments: A re-assessment.
18 *Global Biogeochem. Cycles* 19, 1–7. <https://doi.org/10.1029/2004GB002368>
- 19 Cárcamo, P.J., Hernández-Miranda, E., Veas, R., Quiñones, R.A., 2017. Macrofaunal
20 community structure in Bahía Concepción (Chile) before and after the 8.8 Mw Maule
21 mega-earthquake and tsunami. *Mar. Environ. Res.* 130, 233–247.
22 <https://doi.org/10.1016/j.marenvres.2017.07.022>
- 23 Castaing, P., Allen, G., Houdart, M., Moign, Y., 1979. Étude par télédétection de la dispersion
24 en mer des eaux estuariennes issues de la Gironde et du Pertuis de Maumusson. *Oceanol.*
25 *Acta* 2, 459–468. <https://doi.org/https://archimer.ifremer.fr/doc/00122/23361/>
- 26 Castaing, P., Allen, G.P., 1981. Mechanisms controlling seaward escape of suspended sediment
27 from the Gironde: A macrotidal estuary in France. *Mar. Geol.* 40, 101–118.
28 [https://doi.org/10.1016/0025-3227\(81\)90045-1](https://doi.org/10.1016/0025-3227(81)90045-1)
- 29 Castaing, P., Philipps, I., Weber, O., 1982. Répartition et dispersion des suspensions dans les
30 eaux du plateau continental aquitain. *Oceanol. Acta* 5, 85–96.
31 <https://doi.org/https://archimer.ifremer.fr/doc/00121/23193/>
- 32 Cathalot, C., Rabouille, C., Pastor, L., Deflandre, B., Viollier, E., Buscail, R., Grémare, A.,
33 Treignier, C., Pruski, A., 2010. Temporal variability of carbon recycling in coastal
34 sediments influenced by rivers: Assessing the impact of flood inputs in the Rhône River
35 prodelta. *Biogeosciences* 7, 1187–1205. <https://doi.org/10.5194/bg-7-1187-2010>
- 36 Cathalot, C., Rabouille, C., Tisnérat-Laborde, N., Toussaint, F., Kerhervé, P., Buscail, R.,
37 Loftis, K., Sun, M.Y., Tronczynski, J., Azoury, S., Lansard, B., Treignier, C., Pastor, L.,
38 Tesi, T., 2013. The fate of river organic carbon in coastal areas: A study in the Rhône
39 River delta using multiple isotopic ($\delta^{13}\text{C}$, $\delta^{14}\text{C}$) and organic tracers. *Geochim.*
40 *Cosmochim. Acta* 118, 33–55. <https://doi.org/10.1016/j.gca.2013.05.001>

- 1 Cirac, P., Berne, S., Castaing, P., Weber, O., 2000. Processus de mise en place et d'évolution
2 de la couverture sédimentaire superficielle de la plate-forme nord-aquitaine. *Oceanol.*
3 *Acta* 23, 663–686. [https://doi.org/10.1016/s0399-1784\(00\)00110-9](https://doi.org/10.1016/s0399-1784(00)00110-9)
- 4 Clarke, K.R., Somerfield, P.J., Gorley, R.N., 2008. Testing of null hypotheses in exploratory
5 community analyses: similarity profiles and biota-environment linkage. *J. Exp. Mar. Bio.*
6 *Ecol.* 366, 56–69. <https://doi.org/10.1016/j.jembe.2008.07.009>
- 7 Clarke, K.R., Warwick, R.M., 2001. Change in Marine Communities: An Approach to
8 Statistical Analysis and Interpretation, 2nd edition. PRIMER-E, Plymouth.
- 9 Constantin, S., Doxaran, D., Derkacheva, A., Novoa, S., Lavigne, H., 2018. Multi-temporal
10 dynamics of suspended particulate matter in a macro-tidal river Plume (the Gironde) as
11 observed by satellite data. *Estuar. Coast. Shelf Sci.* 202, 172–184.
12 <https://doi.org/10.1016/j.ecss.2018.01.004>
- 13 Coplen, T.B., 2011. Guidelines and recommended terms for expression of stable- isotope-ratio
14 and gas-ratio measurement results. *Rapid Commun. Mass Spectrom* 25, 2538–2560.
15 <https://doi.org/10.1002/rcm.5129>
- 16 Deflandre, B., 2018a. JERICOBENT-3 cruise, RV Côtes De La Manche.
17 <https://doi.org/10.17600/18000469>
- 18 Deflandre, B., 2018b. JERICOBENT-4 cruise, RV Côtes De La Manche.
19 <https://doi.org/10.17600/18000470>
- 20 Deflandre, B., 2017. JERICOBENT-2 cruise, RV Côtes De La Manche.
21 <https://doi.org/10.17600/17011000>
- 22 Deflandre, B., 2016. JERICOBENT-1 cruise, RV Côtes De La Manche.
23 <https://doi.org/10.17600/16010400>
- 24 Diaz, M., Grasso, F., Le Hir, P., Sottolichio, A., Caillaud, M., Thouvenin, B., 2020. Modeling
25 Mud and Sand Transfers Between a Macrotidal Estuary and the Continental Shelf:
26 Influence of the Sediment Transport Parameterization. *J. Geophys. Res. Ocean.* 125.
27 <https://doi.org/10.1029/2019JC015643>
- 28 Dobbs, F.C., Vozarik, J.M., 1983. Immediate effects of a storm on coastal infauna. *Mar. Ecol.*
29 *Prog. Ser.* 11, 273–279. <https://doi.org/https://doi.org/10.3354/meps011273>
- 30 Doxaran, D., Froidefond, J.M., Castaing, P., Babin, M., 2009. Dynamics of the turbidity
31 maximum zone in a macrotidal estuary (the Gironde, France): Observations from field
32 and MODIS satellite data. *Estuar. Coast. Shelf Sci.* 81, 321–332.
33 <https://doi.org/10.1016/j.ecss.2008.11.013>
- 34 Dubosq, N., Schmidt, S., Walsh, J.P., Grémare, A., Gillet, H., Lebleu, P., Poirier, D., Perello,
35 M.C., Lamarque, B., Deflandre, B., 2021. A first assessment of organic carbon burial in
36 the West Gironde Mud Patch (Bay of Biscay). *Cont. Shelf Res.* 221.
37 <https://doi.org/10.1016/j.csr.2021.104419>
- 38 Etcheber, H., Relexans, J.C., Beliard, M., Weber, O., Buscail, R., Heussner, S., 1999.
39 Distribution and quality of sedimentary organic matter on the Aquitanian margin (Bay of

- Biscay). *Deep. Res. Part II* 46, 2249–2288. [https://doi.org/10.1016/S0967-0645\(99\)00062-4](https://doi.org/10.1016/S0967-0645(99)00062-4)
- Fontugne, M.R., Jouanneau, J.M., 1987. Modulation of the particulate organic carbon flux to the ocean by a macrotidal estuary: Evidence from measurements of carbon isotopes in organic matter from the Gironde system. *Estuar. Coast. Shelf Sci.* 24, 377–387. [https://doi.org/10.1016/0272-7714\(87\)90057-6](https://doi.org/10.1016/0272-7714(87)90057-6)
- Gadel, F., Jouanneau, J.M., Weber, O., Serve, L., Comellas, L., 1997. Traceurs organiques dans les dépôts de la vasière Ouest-Gironde (Golfe de Gascogne). *Oceanol. Acta* 20, 687–695. <https://doi.org/https://archimer.ifremer.fr/doc/00093/20426/>
- Glémarec, M., 1978. Problèmes d'écologie dynamique et de succession en baie de Concarneau. *Vie Milieu* 1–20.
- Goñi, M.A., Ruttenger, K.C., Eglinton, T.I., 1998. A reassessment of the sources and importance of land-derived organic matter in surface sediments from the Gulf of Mexico. *Geochim. Cosmochim. Acta* 62, 3055–3075. [https://doi.org/10.1016/S0016-7037\(98\)00217-8](https://doi.org/10.1016/S0016-7037(98)00217-8)
- Gordon, E.S., Goñi, M.A., Roberts, Q.N., Kineke, G.C., Allison, M.A., 2001. Organic matter distribution and accumulation on the inner Louisiana shelf west of the Atchafalaya River. *Cont. Shelf Res.* 21, 1691–1721. [https://doi.org/10.1016/S0278-4343\(01\)00021-8](https://doi.org/10.1016/S0278-4343(01)00021-8)
- Grasso, F., Verney, R., Le Hir, P., Thouvenin, B., Schulz, E., Kervella, Y., Khojasteh Pour Fard, I., Lemoine, J.P., Dumas, F., Garnier, V., 2018. Suspended Sediment Dynamics in the Macrotidal Seine Estuary (France): 1. Numerical Modeling of Turbidity Maximum Dynamics. *J. Geophys. Res. Ocean.* 123, 558–577. <https://doi.org/10.1002/2017JC013185>
- Grémare, A., Gutiérrez, D., Anschütz, P., Amouroux, J.M., Deflandre, B., Vétion, G., 2005. Spatio-temporal changes in totally and enzymatically hydrolyzable amino acids of superficial sediments from three contrasted areas. *Prog. Oceanogr.* 65, 89–111. <https://doi.org/10.1016/j.pocean.2005.02.016>
- Harmelin-Vivien, M.L., Bănar, D., Dierking, J., Hermand, R., Letourneur, Y., Salen-Picard, C., 2009. Linking benthic biodiversity to the functioning of coastal ecosystems subjected to river runoff (NW Mediterranean). *Anim. Biodivers. Conserv.* 32, 135–145. <https://doi.org/https://doi.org/10.32800/abc.2009.32.0135>
- Harrell, F.E., 2021. Hmisc: Harrell Miscellaneous. R Packag. version 4-5-0.
- Hedges, J.I., Keil, R.G., 1995. Sedimentary organic matter preservation: an assessment and speculative synthesis. *Mar. Chem.* 49, 81–115. [https://doi.org/10.1016/0304-4203\(95\)00008-F](https://doi.org/10.1016/0304-4203(95)00008-F)
- Herbland, A., Delmas, D., Laborde, P., Sautour, B., Artigas, F., 1998. Phytoplankton spring bloom of the Gironde plume waters in the Bay of Biscay: Early phosphorus limitation and food-web consequences. *Oceanol. Acta* 21, 279–291. [https://doi.org/10.1016/S0399-1784\(98\)80015-7](https://doi.org/10.1016/S0399-1784(98)80015-7)
- Hiscock, K., 1984. Rocky shore surveys of the Isles of Scilly. March 27th to April 1st and July 7th to 15th 1983. Peterbrgh. Nat. Conserv. Coun. CSD Rep. 509.

- 1 Jalón-Rojas, I., Sottolichio, A., Hanquiez, V., Fort, A., Schmidt, S., 2018. To what extent
2 multidecadal changes in morphology and fluvial discharge impact tide in a convergent
3 (turbid) tidal river. *J. Geophys. Res. Ocean.* 123, 3241–3258.
4 <https://doi.org/10.1002/2017JC013466>
- 5 Jouanneau, J.M., Weber, O., Latouche, C., Vernet, J.P., Dominik, J., 1989. Erosion, non-
6 deposition and sedimentary processes through a sedimentological and radioisotopic study
7 of surficial deposits from the “Ouest-Gironde vasière” (Bay of Biscay). *Cont. Shelf Res.*
8 9, 325–342. [https://doi.org/10.1016/0278-4343\(89\)90037-X](https://doi.org/10.1016/0278-4343(89)90037-X)
- 9 Keil, R.G., Mayer, L.M., Quay, P.D., Richey, J.E., Hedges, J.I., 1997. Loss of organic matter
10 from riverine particles in deltas. *Geochim. Cosmochim. Acta* 61, 1507–1511.
11 [https://doi.org/10.1016/S0016-7037\(97\)00044-6](https://doi.org/10.1016/S0016-7037(97)00044-6)
- 12 Keil, R.G., Tsamakis, E., Giddings, J.C., Hedges, J.I., 1998. Biochemical distributions (amino
13 acids, neutral sugars, and lignin phenols) among size-classes of modern marine sediments
14 from the Washington coast. *Geochim. Cosmochim. Acta* 62, 1347–1364.
15 [https://doi.org/10.1016/S0016-7037\(98\)00080-5](https://doi.org/10.1016/S0016-7037(98)00080-5)
- 16 Labry, C., Herbland, A., Delmas, D., 2002. The role of phosphorus on planktonic production
17 of the Gironde plume waters in the Bay of Biscay. *J. Plankton Res.* 24, 97–117.
18 <https://doi.org/10.1093/plankt/24.2.97>
- 19 Lamarque, B., Deflandre, B., Dalto, A.G., Schmidt, S., Romero-Ramirez, A., Garabetian, F.,
20 Dubosq, N., Diaz, M., Grasso, F., Sottolichio, A., Bernard, G., Gillet, H., Cordier, M.A.,
21 Poirier, D., Lebleu, P., Derriennic, H., Danilo, M., Tenório, M.M.B., Grémare, A., 2021.
22 Spatial distributions of surface sedimentary organics and sediment profile image
23 characteristics in a high-energy temperate marine riomar: The west gironde mud patch. *J.*
24 *Mar. Sci. Eng.* 9, 242. <https://doi.org/10.3390/jmse9030242>
- 25 Lansard, B., Rabouille, C., Denis, L., Grenz, C., 2009. Benthic remineralization at the land-
26 ocean interface: A case study of the Rhône River (NW Mediterranean Sea). *Estuar. Coast.*
27 *Shelf Sci.* 81, 544–554. <https://doi.org/10.1016/j.ecss.2008.11.025>
- 28 Lazure, P., Dumas, F., 2008. An external-internal mode coupling for a 3D hydrodynamical
29 model for applications at regional scale (MARS). *Adv. Water Resour.* 31, 233–250.
30 <https://doi.org/10.1016/j.advwatres.2007.06.010>
- 31 Lesueur, P., Jouanneau, J.M., Boust, D., Tastet, J.P., Weber, O., 2001. Sedimentation rates and
32 fluxes in the continental shelf mud fields in the Bay of Biscay (France). *Cont. Shelf Res.*
33 21, 1383–1401. [https://doi.org/10.1016/S0278-4343\(01\)00004-8](https://doi.org/10.1016/S0278-4343(01)00004-8)
- 34 Lesueur, P., Tastet, J.P., Weber, O., Sinko, J.A., 1991. Modèle faciologique d’un corps
35 sédimentaire pélitique de plate-forme la vasière Ouest-Gironde (France). *Oceanol. Acta*
36 11, 143–153. <https://doi.org/https://archimer.ifremer.fr/doc/00267/37871/>
- 37 Lesueur, P., Tastet, J.P., 1994. Facies, internal structures and sequences of modern Gironde-
38 derived muds on the Aquitaine inner shelf, France. *Mar. Geol.* 120, 267–290.
39 [https://doi.org/10.1016/0025-3227\(94\)90062-0](https://doi.org/10.1016/0025-3227(94)90062-0)
- 40 Lesueur, P., Tastet, J.P., Marambat, L., 1996. Shelf mud fields formation within historical

- times: Examples from offshore the Gironde estuary, France. *Cont. Shelf Res.* 16, 1849–1870. [https://doi.org/10.1016/0278-4343\(96\)00013-1](https://doi.org/10.1016/0278-4343(96)00013-1)
- Lesueur, P., Tastet, J.P., Weber, O., 2002. Origin and morphosedimentary evolution of fine-grained modern continental shelf deposits: The Gironde mud fields (Bay of Biscay, France). *Sedimentology* 49, 1299–1320. <https://doi.org/10.1046/j.1365-3091.2002.00498.x>
- Levin, L.A., Boesch, D.F., Covich, A., Dahm, C., Erséus, C., Ewel, K.C., Kneib, R.T., Moldenke, A., Palmer, M.A., Snelgrove, P., Strayer, D., Weslawski, J.M., 2001. The function of marine critical transition zones and the importance of sediment biodiversity. *Ecosystems* 4, 430–451. <https://doi.org/10.1007/s10021-001-0021-4>
- Longère, P., Dorel, D., 1970. Etude des sédiments meubles de la vasière de la Gironde et des régions avoisinantes. *Rev. des Trav. l'Institut des Pêches Marit.* 34, 233–256.
- Lotze, H.K., Lenihan, H.S., Bourque, B.J., Bradbury, R.H., Cooke, R.G., Kay, M.C., Kidwell, S.M., Kirby, M.X., Peterson, C.H., Jackson, J.B.C., 2006. Depletion, Degradation, and Recovery Potential of Estuaries and Coastal Seas. *Science*. 312, 1806–1809. <https://doi.org/10.1126/science.1128035>
- Marion, C., Dufois, F., Arnaud, M., Vella, C., 2010. In situ record of sedimentary processes near the Rhône River mouth during winter events (Gulf of Lions, Mediterranean Sea). *Cont. Shelf Res.* 30, 1095–1107. <https://doi.org/10.1016/j.csr.2010.02.015>
- Massé, C., Meisterhans, G., Deflandre, B., Bachelet, G., Bourasseau, L., Bichon, S., Ciutat, A., Jude-Lemeilleur, F., Lavesque, N., Raymond, N., Grémare, A., Garabetian, F., 2016. Bacterial and macrofaunal communities in the sediments of the West Gironde Mud Patch, Bay of Biscay (France). *Estuar. Coast. Shelf Sci.* 179, 189–200. <https://doi.org/10.1016/j.ecss.2016.01.011>
- Masselink, G., Castelle, B., Scott, T., Dodet, G., Suanez, S., Jackson, D., Floc'h, F., 2016. Extreme wave activity during 2013/2014 winter and morphological impacts along the Atlantic coast of Europe. *Geophys. Res. Lett.* 43, 2135–2143. <https://doi.org/10.1002/2015GL067492>.Received
- Mayer, L.M., 1994a. Relationships between mineral surfaces and organic carbon concentrations in soils and sediments. *Chem. Geol.* 114, 347–363. [https://doi.org/10.1016/0009-2541\(94\)90063-9](https://doi.org/10.1016/0009-2541(94)90063-9)
- Mayer, L.M., 1994b. Surface area control of organic carbon accumulation in continental shelf sediments. *Geochim. Cosmochim. Acta* 58, 1271–1284. [https://doi.org/10.1016/0016-7037\(94\)90381-6](https://doi.org/10.1016/0016-7037(94)90381-6)
- Mayer, L.M., Linda L., S., Sawyer, T., Plante, C.J., Jumars, P.A., Sel, R.L., 1995. Bioavailable amino acids in sediments: A biomimetic, kinetics based approach. *Limnol. Oceanogr.* 40, 511–520. <https://doi.org/10.4319/lo.1995.40.3.0511>
- McKee, B.A., Aller, R.C., Allison, M.A., Bianchi, T.S., Kineke, G.C., 2004. Transport and transformation of dissolved and particulate materials on continental margins influenced by major rivers: Benthic boundary layer and seabed processes. *Cont. Shelf Res.* 24, 899–

926. <https://doi.org/10.1016/j.csr.2004.02.009>

Medernach, L., Grémare, A., Amoureux, J.M., Colomines, J.C., Vétion, G., 2001. Temporal changes in the amino acid contents of particulate organic matter sedimenting in the Bay of Banyuls-sur-Mer (northwestern Mediterranean). *Mar. Ecol. Prog. Ser.* 214, 55–65. <https://doi.org/10.3354/meps214055>

Miralles, J., Radakovitch, O., Aloisi, J.C., 2005. ²¹⁰Pb sedimentation rates from the Northwestern Mediterranean margin. *Mar. Geol.* 216, 155–167. <https://doi.org/10.1016/j.margeo.2005.02.020>

Neveux, J., Lantoiné, F., 1993. Spectrofluorometric assay of chlorophylls and phaeopigments using the least squares approximation technique. *Deep. Res. Part I* 40, 1747–1765. [https://doi.org/10.1016/0967-0637\(93\)90030-7](https://doi.org/10.1016/0967-0637(93)90030-7)

Oksanen, J., Blanchet, F.G., Friendly, M., Kindt, R., Legendre, P., McGlinn, D., Minchin, P.R., O'Hara, R.B., Simpson, G.L., Solymos, P., Stevens, M.H.H., Szoecs, E., Wagner, H., 2019. *vegan: Community Ecology Package*. R Packag. version 2-5-6.

Parra, M., Castaing, P., Jouanneau, J.M., Grousset, F., Latouche, C., 1998. Nd-Sr isotopic composition of present-day sediments from the Gironde Estuary, its draining basins and the WestGironde mud patch (SW France). *Cont. Shelf Res.* 19, 135–150. [https://doi.org/10.1016/S0278-4343\(98\)00083-1](https://doi.org/10.1016/S0278-4343(98)00083-1)

Pastor, L., Deflandre, B., Viollier, E., Cathalot, C., Metzger, E., Rabouille, C., Escoubeyrou, K., Lloret, E., Pruski, A.M., Vétion, G., Desmalades, M., Buscail, R., Grémare, A., 2011. Influence of the organic matter composition on benthic oxygen demand in the Rhône River prodelta (NW Mediterranean Sea). *Cont. Shelf Res.* 31, 1008–1019. <https://doi.org/10.1016/j.csr.2011.03.007>

Pastor, L., Rabouille, C., Metzger, E., Thibault de Chanvalon, A., Viollier, E., Deflandre, B., 2018. Transient early diagenetic processes in Rhône prodelta sediments revealed in contrasting flood events. *Cont. Shelf Res.* 166, 65–76. <https://doi.org/10.1016/j.csr.2018.07.005>

Pearson, T.H., Rosenberg, R., 1978. Macrobenthos succession in relation to organic enrichment and pollution of the marine environment. *Oceanogr. Mar. Biol. Annu. Rev.* 16, 229–331.

Picton, B.E., Emblow, C.S., Morrow, C.C., Sides, E.M., Costello, M.J., 1994. Marine communities of the Mulroy Bay and Lough Swill area, north-west Ireland, with an assessment of their nature conservation importance. *Environ. Sci. Unit, Trinity Coll. (f. Surv. Report)*.

R Core Team, 2019. *R: A Language and Environment for Statistical Computing*. R Foundation for Statistical Computing, Vienna, Austria. <https://www.R-project.org/>.

Rees, E.I.S., Nicholaidou, A., Laskaridou, P., 1977. The Effects of Storms on the Dynamics of Shallow Water Benthic Associations. *Biol. Benthic Org.* 465–474. <https://doi.org/10.1016/b978-0-08-021378-1.50052-x>

Relexans, J.C., Lin, R.G., Castel, J., Etcheber, H., Laborde, P., 1992. Response of biota to sedimentary organic matter quality of the west Gironde mud patch, Bay of Biscay

- (France). *Oceanol. Acta* 15, 639–649.
<https://doi.org/https://archimer.ifremer.fr/doc/00101/21231/>
- Rhoads, D.C., Boesch, D.F., Zhican, T., Fengshan, X., Liqiang, H., Nilsen, K.J., 1985. Macrobenthos and sedimentary facies on the Changjiang delta platform and adjacent continental shelf, East China Sea. *Cont. Shelf Res.* 4, 189–213.
[https://doi.org/10.1016/0278-4343\(85\)90029-9](https://doi.org/10.1016/0278-4343(85)90029-9)
- Roland, A., Ardhuin, F., 2014. On the developments of spectral wave models: Numerics and parameterizations for the coastal ocean. *Ocean Dyn.* 64, 833–846.
<https://doi.org/10.1007/s10236-014-0711-z>
- Soulsby, R., 1997. *Dynamics of Marine Sands: A Manual for Practical Applications*, Thomas Tel. ed.
- Tesi, T., Miserocchi, S., Goñi, M.A., Langone, L., 2007. Source, transport and fate of terrestrial organic carbon on the western Mediterranean Sea, Gulf of Lions, France. *Mar. Chem.* 105, 101–117. <https://doi.org/10.1016/j.marchem.2007.01.005>
- Ulses, C., Estournel, C., Durrieu de Madron, X., Palanques, A., 2008. Suspended sediment transport in the Gulf of Lions (NW Mediterranean): Impact of extreme storms and floods. *Cont. Shelf Res.* 28, 2048–2070. <https://doi.org/10.1016/j.csr.2008.01.015>
- Wakeham, S.G., Lee, C., Hedges, J.I., Hernes, P.J., Peterson, M.L., 1997. Molecular indicators of diagenetic status in marine organic matter. *Geochim. Cosmochim. Acta* 61, 5363–5369.
<https://doi.org/10.5833/jjgs.33.70>
- Weber, O., Jouanneau, J.M., Ruch, P., Mirmand, M., 1991. Grain-size relationship between suspended matter originating in the Gironde estuary and shelf mud-patch deposits. *Mar. Geol.* 96, 159–165. [https://doi.org/10.1016/0025-3227\(91\)90213-N](https://doi.org/10.1016/0025-3227(91)90213-N)
- Wheatcroft, R.A., 2006. Time-series measurements of macrobenthos abundance and sediment bioturbation intensity on a flood-dominated shelf. *Prog. Oceanogr.* 71, 88–122.
<https://doi.org/10.1016/j.pcean.2006.06.002>
- Worm, B., Barbier, E.B., Beaumont, N., Duffy, J.E., Folke, C., Halpern, B.S., Jackson, J.B.C., Lotze, H.K., Micheli, F., Palumbi, S.R., Sala, E., Selkoe, K.A., Stachowicz, J.J., Watson, R., 2006. Impacts of biodiversity loss on ocean ecosystem services. *Science* 314, 787–790. <https://doi.org/10.1126/science.1132294>
- Zuo, Z., Eisma, D., Berger, G.W., 1991. Determination of sediment accumulation and mixing rates in the Gulf of Lions, Mediterranean Sea. *Oceanol. Acta* 14, 253–262.
<https://doi.org/https://archimer.ifremer.fr/doc/00101/21255/>